PROTEIN PRENYLATION INHIBITORS REVEAL A NOVEL ROLE FOR RHOA AND RHOC IN TRAFFICKING OF G PROTEIN-COUPLED RECEPTORS THROUGH RECYCLING ENDOSOMES

A Dissertation
Presented to
The Academic Faculty

by

Paul David Salo

In Partial Fulfillment
of the Requirements for the Degree
Doctor of Philosophy in the
School of Chemistry and Biochemistry

Georgia Institute of Technology
December 2007

This dissertation contains the following errata substitutions to the original document:

Errata Page 2 for original page 1.

Errata Page 3 – 16 for original pages 3-28.

Errata page 17 – 19 for original pages 69 – 71.

PROTEIN PRENYLATION INHIBITORS REVEAL A NOVEL ROLE FOR RHOA AND RHOC IN TRAFFICKING OF G PROTEIN-COUPLED RECEPTORS THROUGH RECYCLING ENDOSOMES

Approved by:

Dr. Nicholas Hud, Co-Advisor
School of Chemistry and Biochemistry
Georgia Institute of Technology

Dr. Donald Doyle
School of Chemistry and Biochemistry
Georgia Institute of Technology

Dr. Christoph Fahrni
School of Chemistry and Biochemistry
Georgia Institute of Technology

Dr. Nael McCarty
School of Biology
Georgia Institute of Technology

Dr. Harish Radhakrishna, Co-Advisor
Strategic Research Department
The Coca-Cola Company

Date Approved: August 10, 2007

ACKNOWLEDGEMENTS

I would like to thank the following members of the former Radhakrishna Lab for numerous helpful discussions during the course of this project: Dr. Nikhil Urs, Dr. Kymry Jones, and Jennifer Hurst-Kennedy. I would especially like to thank Dr. Urs for all of his assistance during the course of this project. I thank all of my committee members, Dr. Nicholas Hud, Dr. Harish Radhakrishna, Dr. Christoph Fahrni, Dr. Donald Doyle, and Dr. Nael McCarty, for their time and attention. I specifically thank Dr. Radhakrishna for continuing to supervise my research and mentor me, even after taking a position in private industry. This research would not have been possible without Dr. Radhakrishna. I also specifically thank Dr. McCarty for being extra supportive after Dr. Radhakrishna's departure from Georgia Tech.

I thank Dr. Fred Maxfield (Weill Medical College of Cornell University, New York, NY) for generously supplying Alexa 546-transferrin.

This work was supported by National Institutes of Health grant HL 67134 to Dr. Harish Radhakrishna. I was supported by a National Science Foundation Integrative Graduate Education and Research Traineeship (NSF IGERT-0221600).

TABLE OF CONTENTS

LIST OF TABLES

LIST OF FIGURES

LIST OF ABBREVIATIONS

$[Ca^{2+}]_i$	Intracellular Ca^{2+} concentration
ADP	Adenosine diphosphate
AP-2	Adapter protein-2
ARF	ADP-ribosylation factor
ARH	Autosomal recessive hypercholesterolemia
ATP	Adenosine 5'-triphosphate
CCP	Clathrin-coated pit
Cdc42	Cell division cycle 42
EBP50	Ezrin-radixin-moesin-binding phosphoprotein of 50 kDa
EEA1	Early endosomal autoantigen 1
EH	Eps15 homology
EHD1	EH-domain containing 1
EM	Electron microscopy
Eps15	Epidermal growth factor receptor pathway substrate 15
ER	Endoplasmic reticulum
ERC	Endocytic recycling compartment
ERK	Extracellular signal–regulated kinase
FDA	Food and Drug Administration
FH	Familial hypercholesterolemia
FOH	Farnesol
FPP	Farnesylpyrophosphate
FTase	Farnesyltransferase
G protein	Guanine nucleotide binding protein

GASP	G protein–coupled receptor–associated sorting protein
GDP	Guanosine diphosphate
GGOH	Geranylgeraniol
GGPP	Geranylgeranylpyrophosphate
GGTase I	Geranylgeranyltransferase I
GPCR	G protein-coupled receptor
GRK	G protein receptor kinase
GTP	Guanosine triphosphate
HAT	Histone acetyltransferase
HDAC1	Histone deacetylase 1
HeLa	Henrietta Lacks
HIP	Hsc/Hsp interacting protein
HMG-CoA	3-hydroxy-3-methylglutaryl-Coenzyme A
HRS	Hepatocyte growth factor–regulated tyrosine kinase substrate
Icmt	Isoprenylcysteine carboxyl methyltransferase
kDa	Kilodalton
LPA	Lysophosphatidic acid (18:1; 1-oleoyl-2-hydroxy-*sn*-glycero-3-phosphate)
LPP	Lipid phosphate phosphatase
MAP	Mitogen-activated protein
MAR	Matrix associated region
NHERF	Na^+/H^+ exchanger regulatory factor
NSF	*N*-ethylmaleimide-sensitive factor
PDGF	Platelet-derived growth factor
PI3K	Phosphatidylinositol 3-kinase
PPARγ	Peroxisome proliferator-activated receptor-γ

Rac1	Ras-related C3 botulinum toxin substrate 1
Ras	Rat sarcoma
Rce1	Ras converting enzyme 1
RhoA	Ras homolog gene family, member A
RhoB	Ras homolog gene family, member B
RhoC	Ras homolog gene family, member C
RME	Rat MAR element
ROCK	Rho kinase
S1P	Sphingosine 1-phosphate
SNX1	Sorting nexin 1
vps	Vacuolar protein–sorting

SUMMARY

The following research was undertaken to elucidate the mechanism by which statin drugs (HMG-CoA reductase inhibitors) cause the sequestration of G protein-coupled receptors (GPCRs) in the endocytic recycling compartment (ERC). Specifically, we examined the effects of statin drugs on the trafficking of the LPA_1 lysophosphatidic acid receptor (LPA_1R).

Membrane trafficking of GPCRs, to and from the plasma membrane, regulates their surface abundance, which in turn, contributes to the sensitivity of cells towards agonists. Although much is known about the internalization and desensitization of GPCRs, very little is known about the recycling of GPCRs from endosomes back to the plasma membrane. LPA_1Rs are normally present on the surface of the cell. After binding to lysophosphatidic acid (LPA), the receptor tranduces the signal to heterotrimeric G proteins present inside the cell. These G proteins then activate downstream signaling pathways within the cell that result in effects, such as the stimulation of cell proliferation. The LPA_1R is then internalized to early endosomes, and then transits to recycling endosomes from which it is normally recycled back to the cell surface.

Our initial findings were that HMG-CoA reductase inhibitors (atorvastatin and mevastatin) induce the sequestration of the G protein-coupled LPA_1R in recycling endosomes, most likely by inhibiting the recycling of tonically (in the absence of LPA stimulation) internalized receptors. Atorvastatin also induced sequestration of β_2-adrenergic receptors and M_2 muscarinic acetylcholine receptors. Whereas, co-addition of

geranylgeranylpyrophosphate (GGPP) or geranylgeraniol (GGOH) prevented atorvastatin-induced sequestration of LPA_1Rs, the geranylgeranyltransferase-I inhibitor, GGTI-298, mimicked atorvastatin and induced LPA_1R sequestration. This suggested that statin-induced endosomal sequestration was caused by defective protein prenylation. The likely targets of atorvastatin and GGTI-298 are the Rho family GTPases, RhoC and RhoA, since both inhibitors greatly reduced the abundance of these GTPases and since knockdown of endogenous RhoC or RhoA with small interfering RNAs (siRNAs) led to endosomal sequestration of LPA_1R. Knockdown of RhoC was much more potent at inducing endosomal sequestration than knockdown of either RhoA or RhoB. In contrast, atorvastatin, GGTI-298, siRNA against RhoA, B, or C did not alter the internalization or recycling of transferrin receptors, indicating that recycling of transferrin receptors is distinct from LPA_1Rs. Thus, these results, for the first time, implicate RhoA and RhoC in endocytic recycling of LPA_1Rs and identify atorvastatin and GGTI-298 as novel inhibitors of this process.

Future studies will likely reveal specific effector proteins that interact with RhoA and RhoC. These effectors may be involved with sorting the receptors, pinching off transport vesicles, or tethering the vesicles to motor proteins that will transport them back to the cell surface.

CHAPTER 1

INTRODUCTION

G protein-coupled receptors (GPCRs)

Background on GPCRs

The largest group of signaling receptors in mammalian cells is the G protein-coupled receptors (GPCRs). GPCRs participate in a wide variety of physiological processes including sensing of the external environment (including sight, smell, and taste), neurotransmission, muscle contraction, and mitogenesis (Lefkowitz, 2000). GPCRs undergo a conformational change upon binding to a ligand, which leads to association with and activation of heterotrimeric G proteins (Figure 1, Step 1). In Step 2, desensitization limits the extent of G protein stimulation, wherein most GPCRs are rapidly phosphorylated by G protein receptor kinases (GRKs) or by second messenger kinases (Benovic *et al.*, 1987). β-arrestins bind to the GRK-phosphorylated GPCRs and block G proteins from interacting with and binding to the desensitized GPCR (Figure 1, Step 2) (Ahn *et al.*, 2003). Most GPCRs are then transported into cells through endocytic pathways (Figure 1, Step 3) and proceed to early endosomes from which they are either sorted to lysosomes for degradation (down-regulation; Figure 1, Step 4) or are de-phosphorylated and transported to recycling endosomes to be recycled back to the plasma membrane for further signaling (resensitization; Figure 1, Step 5) (Lin *et al.*, 2001; Zhang *et al.*, 1997). Many GPCRs undergo a low basal rate of endocytosis and recycling even in the absence of stimulating ligands (Ferguson, 2001).

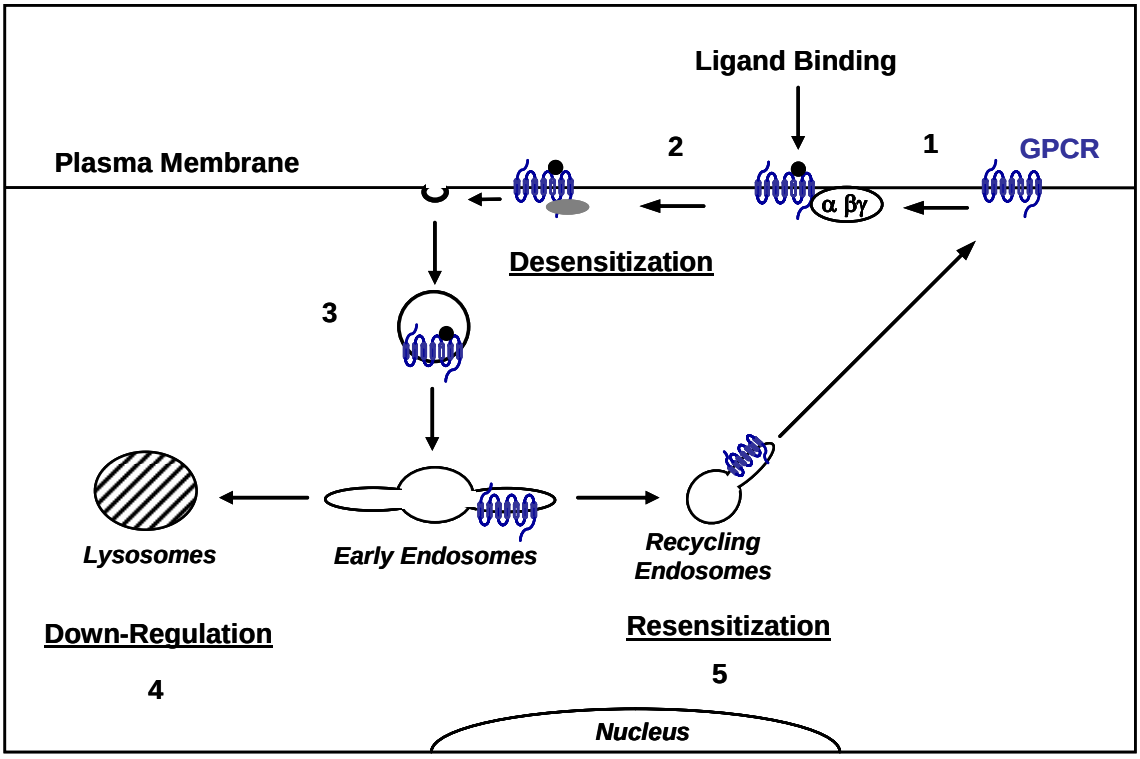

Figure 1: Overall model of GPCR regulation.
(1) Ligand binding and activation of heterotrimeric G proteins. (2) β-arrestin binding and desensitization. (3) Endocytosis. (4) Degradation in lysosomes (down-regulation). (5) Recycling back to the plasma membrane for further signaling (resensitization).

There are over 800 genes in the human genome that encode GPCRs, and although many studies have been performed there is much that is yet to be discovered about the detailed functional mechanisms of GPCRs (Wolfe and Trejo, 2007). The structure of the GPCR comprises an extracellular N-terminal domain, seven transmembrane domains connected by three intracellular and three extracellular loops, and an intracellular C-terminal domain (Pitcher *et al.*, 1998). The complex structures of GPCRs allow these versatile receptors to recognize and interact with a wide variety of molecules both within the cell and outside the cell.

GPCR endocytic trafficking overview

The movement of GPCRs through the cell is a complex process with delicate regulation. The pathways for endocytosis can be divided into three main categories, clathrin-dependent endocytosis, caveolae-dependent endocytosis, and finally other pathways that are independent of both clathrin and caveolae. The first type of endocytosis discovered was clathrin-dependent endocytosis, in which vesicles coated with clathrin bud from and are pinched off from the cell surface. The clathrin coats have a role in packaging the GPCRs or other cargo while also providing a structural shape to the vesicle. Thus, there is a connection between the sorting of the cargo and the packaging of the cargo in clathrin-dependent endocytosis (Schmid, 1997).

The proper functioning of GPCRs depends on precise and well controlled membrane trafficking. GPCR trafficking controls processes including receptor down-regulation, receptor internalization, receptor signaling from intracellular compartments, and receptor resensitization via recycling to the plasma membrane from endosomes (Ferguson, 2001). GPCRs are rapidly desensitized after agonist stimulation through

mechanisms involving receptor phosphorylation and, in many cases, through association with the multi-functional scaffolding proteins, β-arrestins (Benovic *et al.*, 1987; Zhang *et al.*, 1997). The internalization of many GPCRs occurs through both clathrin-independent endocytosis and clathrin-dependent endocytosis. After leaving the early endosomes, GPCRs are either sorted to lysosomes for degradation (down-regulation) or can be dephosphorylated and recycled back to the plasma membrane via recycling endosomes. Lysosomal sorting of GPCRs is signaled for by ubiquitylation of the receptors (Shenoy et al., 2001; Shenoy and Lefkowitz, 2003). Some GPCRs that have type I PDZ binding domains in their cytoplasmic tails are sorted for rapid recycling by binding to their target PDZ-containing proteins (Cao *et al.*, 1999; Gage *et al.*, 2005). However, not all GPCRs have PDZ binding domains, so other methods of GPCR recycling must be occurring.

There are two main endocytic recycling pathways (Maxfield and McGraw, 2004). The first, 'fast', pathway is responsible for recycling of proteins from early endosomes to the plasma membrane and is regulated by the small GTPase, Rab4 (van der Sluijs *et al.*, 1992). The second, 'slow', pathway routes proteins through pericentriolar recycling endosomes on their way back to the plasma membrane (Sheff *et al.*, 1999; Maxfield and McGraw, 2004). The recycling endosomes also serve as a direct access point for endocytic cargo to the *trans*-Golgi network (TGN) and to the secretory pathway (Ghosh *et al.*, 1998; Mallard *et al.*, 1998). Recycling endosomes are normally identified by the presence of transferrin receptor (TfnR) and the lack of other cargo, such as low density lipoprotein, which is destined for degradation in lysosomes (Sheff *et al.*, 1999; Maxfield and McGraw, 2004).

Clathrin-dependent endocytosis

Most receptors at the cell surface are internalized through clathrin-dependent endocytosis pathways. Clathrin heavy-chain and clathrin light-chain molecules form a structural framework for the clathrin-coated pit, which is then pinched off from the cell surface plasma membrane by dynamin. The assembly of the clathrin-coated pit is facilitated by various accessory proteins and adaptor proteins, which act to sort specific cargo into the clathrin-coated vesicle. Adapter protein-2 (AP-2) is one of the key adaptors for clathrin-coated vesicles. AP-2 recognizes short dileucine-based and tyrosine-based portions of proteins, but other signals also guide proteins into clathrin-coated vesicles, which implicate additional adaptors sorting distinct cargo into the pathway (Wolfe and Trejo, 2007).

A high level of regulation of clathrin adaptors is indicated in part by observations that the adaptor proteins are themselves ubiquitinated and phosphorylated. Non-visual arrestins were the first adaptors identified with an involvement in clathrin-dependent endocytosis. AP-2 and clathrin interact with non-visual arrestins in the endocytosis of desensitized GPCRs. Two non-visual arrestins, β-arrestin1 and β-arrestin2, are key participants in the clathrin-dependent endocytosis of GPCRs. The binding of β-arrestin1 and β-arrestin2 to desensitized GPCRs displaces the G proteins and aids in the formation of clathrin-coated pits. β-arrestin1 and β-arrestin2 have an amino-terminal antiparallel β-sheet region connected by a core of 12 polar amino acids to a carboxy-terminal antiparallel β-sheet region. The polar amino acids of the core interact with the phosphorylated portions of the desensitized GPCR. GPCR binding exposes the carboxy-

terminal antiparallel β-sheet region that interacts with the heavy-chain of clathrin (Wolfe and Trejo, 2007).

Two major classes of GPCRs

There are two major classes of GPCRs, class A receptors and Class B receptors. Class A receptors bind to β-arrestin2 more strongly than to β-arrestin1, and class A receptors do not interact with visual arrestins. Some examples of class A receptors are dopamine D1A receptors, α1b adrenergic receptors, mu opioid receptors, β2 adrenergic receptors, and endothelin type A receptors. Class B receptors bind to both β-arrestin2 and β-arrestin1 with equally high strength, and class B receptors do interact with visual arrestins. Some examples of class B receptors are substance P receptors, vasopressin V2 receptors, angiotensin II type 1A receptors, thyrotropin-releasing hormone receptors, and neurotensin receptor 1. It was found that swapping the carboxyl-terminal segments of class A receptors and class B receptors also completely switched their respective binding affinities. It was also found that, swapping the carboxyl-terminal segments of β-arrestin2 and β-arrestin1 swapped their cellular localization and swapped their binding affinity for class A receptors. Furthermore, it was shown that GPCRs other than rhodopsin can interact with visual arrestins. These observations point to the signaling of GPCRs being differentially regulated depending on the relative amounts of different arrestins and the interactions of other proteins with the different arrestins (Oakley *et al.*, 2000).

GPCR structural features and interactions

Relatively short sequences in the cytosolic portions of GPCRs predominately facilitate their trafficking to endosomes and lysosomes. Distinct protein coat components are targeted to distinct sequences present in GPCRs. Adaptor proteins AP-1, -2, -3, and -

4, bind to the sequences [DE]XXXL[LI] and YXXO. NPXY sequences interact with AP-2, clathrin, and Dab2 (disabled homolog 2, mitogen-responsive), and AP-2 subunit mu2 interacts with the sequences DXXLL and YXXO. The binding of these target sequences can be further modulated by the sequences being ubiquitinated or phosphorylated. Ubiquitinated GPCRs are trafficked to the lysosomes for degradation (Bonifacino and Traub, 2003).

LPA (lysophosphatidic acid) and LPA receptors

General properties of LPA

Lysophosphatidic acid (LPA) (1-acyl-2-lyso-*sn*-glycero-3-phosphate) is a naturally occurring phospholipid growth factor that comprises a lone fatty acyl chain attached to a backbone of glycerol bound to a phosphate group (van Leeuwen *et al.*, 2003). LPA stimulates specific G protein coupled receptors (GPCRs), which then activate the G_i, G_q, and $G_{12/13}$ families of heterotrimeric G proteins (Ishii *et al.*, 2000). Some of the intracellular processes stimulated by LPA include: intracellular calcium release (Jalink *et al.*, 1995), activation of the Rho GTPase (Ridley and Hall, 1992), transcriptional activation of serum-responsive genes (Hill *et al.*, 1995), and activation of the MAP kinase cascade (van Corven *et al.*, 1992). At the cellular level, LPA can stimulate processes as diverse as neurite retraction (Ishii *et al.*, 2000), smooth muscle contraction (Toews *et al.*, 1997), and cell proliferation. LPA was first shown to stimulate the proliferation of fibroblasts in a G-protein dependent fashion (van Corven *et al.*, 1992). In addition to fibroblasts, LPA potently stimulates the growth of a variety of tumor cells including cells derived from: ovarian cancer (Xu *et al.*, 1995), prostate cancer (Kue *et al.*,

2002), and breast cancer (Xu *et al.*, 1995). The many responses to LPA are mediated by specific receptors for LPA.

LPA production and degradation

LPA can be produced multiple ways within the cell. One method for the production of LPA involves phospholipase A1 or A2 (PLA1 or PLA2) processing phosphatidic acid by removing a fatty acyl chain. Cleavage of fatty acids at the sn-1 position of a phospholipid is performed by PLA1, whereas cleavage of fatty acyl chains at the sn-2 position of a phospholipid is performed by PLA2. The 125 kDa transmembrane protein ATX/lyso phospholipase D (ATX/lysoPLD) was first discovered as an autocrine motility factor produced by human melanoma cells. ATX/lysoPLD can generate LPA from membrane phosphatidylcholine by the removal of choline. Several cancers have been observed to have increased ATX/lysoPLD levels compared to normal cells, such as neuroblastoma, hepatocellular carcinoma, mammary carcinoma, renal-cell carcinoma, and non-small-cell lung carcinoma. The finding that secreted ATX/lysoPLD is a tumor motility factor increases the understanding of the involvement of LPA in cancer progression and initiation (Mills and Moolenaar, 2003).

In order to maintain the delicate balance of a properly functioning cell, the production of LPA needs to be complimented with pathways for LPA degradation. One possible partial control mechanism is that LPA production by ATX/lysoPLD is very well controlled, so as not to allow LPA concentrations to exceed necessary levels in the first place. However, degradation of LPA is a much more direct counterbalance to LPA production. LPA is quickly dephosphorylated and converted to monoacylglycerol. Lipid phosphate phosphohydrolases (LPPs) are integral membrane proteins that

dephosphorylate LPA. At least four LPPs have been identified, and each has six transmembrane segments. Not surprisingly, the expression of LPPs is observed to be lower in ovarian cancer cells compared to normal cells. Thus, increasing LPP expression could be useful as an anti-cancer treatment for ovarian cancer and other cancers that may have decreased LPP expression (Mills and Moolenaar, 2003).

LPA receptors

The first LPA receptor was cloned from a screen for heptahelical receptors that were enriched in embryonic brain cortex; this receptor is now known as LPA_1R and is the most widely expressed LPA receptor (Ishii *et al.*, 2000). In addition to LPA_1R, two other closely-related LPA-specific receptors, LPA_2R and LPA_3R, the more distantly-related LPA_4R, and the recently characterized LPA_5R, comprise the known heptahelical LPA receptors (Lee *et al.*, 2006). It has also been shown that the nuclear receptor PPAR-γ is a high affinity LPA receptor (Mills and Moolenaar, 2003).

The variety of downstream signaling effects of LPA is due to the ability of LPA receptors, specifically LPA_1R, LPA_2R, and LPA_3R to interact with three different G proteins, G_i, G_q, and $G_{12/13}$. Activation of G_i feeds into three main signaling pathways, stimulation of phosphatidylinositol 3-kinase (PI3K), activation of Ras-mitogen-activated protein kinase (Ras-MAPK), and inhibition of adenylyl cyclase that results in decreased cyclic AMP concentration within the cell. Activation of G_q subsequently activates phospholipase C (PLC). Activation of PLC results in the hydrolysis of phosphatidylinositol-bisphosphate and generates second messengers that change the concentration of calcium in the cytosol and activate protein kinase C (PKC). Activation of $G_{12/13}$ results in the activation of RhoA (Mills and Moolenaar, 2003).

LPA_1R and LPA_2R were found to mediate cell rounding induced by LPA, whereas LPA_3R was found to result in neurite elongation in B103 neuroblastoma cells and actually inhibited cell rounding in TR mouse neuroblastoma cells. LPA_1R, LPA_2R, and LPA_3R were found to mediate inhibition of adenylyl cyclase and to mediate PLC activation. In addition, LPA_1R, LPA_2R, and LPA_3R were found to mediate arachidonic acid release and MAPK activation (Ishii *et al.*, 2000).

Although LPARs have been well studied, relatively little is known about the cellular mechanisms that regulate the number of LPA receptors present on the surface plasma membrane of cells.

Prenylated proteins

Overview of prenylation

Proteins, including RhoA, B, and C, that contain a carboxyl-terminal CAAX box (wherein CAAX represents a chain of a cysteine, an aliphatic amino acid, an aliphatic amino acid, and any amino acid) require posttranslational processing to facilitate proper function and localization (Adamson *et al.*, 1992). Prenylation is the process by which proteins are covalently modified with a hydrophobic chain of prenyl (3-methylbut-2-en-1-yl) groups that facilitate interactions with membranes and mediate interactions with other proteins (Casey and Seabra, 1996). RhoC and A are geranylgeranylated by geranylgeranyltransferase type-I (GGTase-I) (Collisson *et al.*, 2003; Casey and Seabra, 1996).

Rho proteins

RhoA, B, and C are members of the Rho family of GTPases. The Rho family of GTPases also encompasses Cdc42 and Rac1. Cdc42 (cell division cycle 42) regulates cell signaling pathways that control a variety of cellular functions including endocytosis, cell migration, cell morphology, and cell cycle progression. Cdc42 regulates the bipolar attachment of spindle microtubules to kinetochores during metaphase of the cell cycle. Cdc42 also is involved in the formation and extension of filopodia, which are thin, actin-rich surface projections that pull migrating cells forward (Bishop and Hall, 2000). Rac1 (Ras-related C3 botulinum toxin substrate 1) is ubiquitously expressed and regulates a variety of cellular functions including cell adhesion, cell differentiation, cytoskeletal reorganization, the control of cell growth, and the activation of protein kinases (Hajdo-Milasinovic *et al.*, 2007).

The rho genes were first identified from a cDNA library of the sea slug *Aplysia*. The homology between *Aplysia* and human Rho proteins was found to be greater than 85%. The rho gene products and ras gene products both have segments of strong internal homology, both are approximately 21 kDa, and both possess carboxy-terminus sequences required for membrane attachment. These similarities suggest that Rho and Ras may have common functions, but may carry out those functions through different mechanisms (Madaule and Axel, 1985). The three human Rho proteins were later denoted RhoA, B, and C, and it was found that all three are modified by C3 transferase from *C. botulinum*. An early study found that microinjection of RhoA into fibroblasts resulted in an increase in actin stress fibers (Ridley, 2001). Interestingly, it was found that LPA is a serum

component that is responsible for Rho-mediated stress fiber formation (Ridley and Hall, 1992).

The localization, trafficking, and functioning of the ras family of proteins relies on modifications to the proteins made after translation. The CAAX box (wherein CAAX represents a chain of a cysteine, an aliphatic amino acid, an aliphatic amino acid, and any amino acid) of the ras proteins can be carboxymethylated or prenylated. RhoA, B, and C are members of the ras family and are carboxymethylated at the carboxy-terminus. RhoB is modified with farnesyl (15 carbon) or geranylgeranyl (20 carbon) groups. A mutation in the CAAX box of p21rhoB of the cysteine at 193 prevented prenylation. Additional mutational studies of p21rhoB found that sites at cysteine 189 and cysteine 192 found that those locations are necessary for palmitoylation (Adamson *et al.*, 1992).

The three human Rho genes were found to be located on separate chromosomes, with RhoA found on 3p21, RhoB found on 2p12, and RhoC found on 5q31 (Cannizzaro *et al.*, 1990). A later study determined that the gene for RhoC was likely generated by an incomplete duplication of the gene for RhoA. It was also determined that the gene for RhoB was likely the result of reverse transcription (Karnoub *et al.*, 2004). RhoB was shown to be a rather unstable protein. In HeLa cells and PC12 (rat adrenal medulla pheochromocytoma) cells, RhoB production is rapidly and transiently induced and varies throughout the stages of the cell cycle. The relative amount of RhoB present peaks during synthesis phase (S-phase) of the cell cycle, and then decreases during the transition from S-phase to Gap 2 (G_2) and mitosis (M) phases of the cell cycle. In addition, a perinuclear localization was observed for growth factor induced RhoB protein.

These findings indicated that RhoB is involved in S-phase and/or in the transition between Gap 1 (G_1) phase and S-phase of the cell cycle (Zalcman *et al.*, 1995).

Guanine nucleotide exchange factors (GEFs) stimulate the exchange of GDP for GTP to generate the active forms of RhoA, B, and C that then interact with effectors and other downstream targets. This downstream communication is then turned off by GTPase activating proteins (GAPs) that stimulate deactivation of RhoA, B, and C. The relative number of Rho GEFs has been found to exceed the number of Rho proteins by a factor of three. It is possible that different receptors utilize different GEFs to activate a specific GTPase. This indicates that a specific GEF links many different receptors to the activation of Rho proteins. Deletions and rearrangements of genes encoding Rho GEFs have been identified in cases of cancer, neurodegenerative disorders, and developmental disorders. The cytosolic or membrane localization of RhoA, B, and C is regulated by guanine nucleotide dissociation inhibitors (GDIs). Inactive (GDP-bound) Rho proteins have a cytosolic localization and are bound to Rho GDIs. For activation of the Rho protein to occur, the Rho GDI must be released from the Rho protein (Schmidt and Hall, 2002).

Pharmacological agents that affect prenylation

HMG-CoA reductase inhibitors (statins)

The statins are a class of compounds that inhibit HMG-CoA reductase and are mainly used to lower blood cholesterol concentrations (Veillard and Mach, 2002). Statins inhibit the rate limiting step of the cholesterol synthesizing mevalonate pathway, which also yields ubiquinones, dolichols, sterol, farnesylpyrophosphate (FPP), and geranylgeranylpyrophosphate (GGPP) (Chan *et al.*, 2003). Atorvastatin, a widely

prescribed statin marketed by Pfizer as Lipitor, was found to inhibit the activation of Rho proteins and inhibit metastasis of melanoma cells exhibiting RhoC overexpression (Collisson *et al.*, 2003).

Geranylgeranyltransferase and Farnesyltransferase Inhibitors (GGTIs and FTIs)

GGTI-298 and FTI-277 are compounds that mimic the CAAX box protein sequence. GGTI-298 inhibits geranylgeranyltransferase I (GGTase I) and FTI-277 inhibits farnesyltransferase (FTase) (Lerner *et al.*, 1995; Vogt *et al.*, 1996). The compound FTI-277 is a potent inhibitor of oncogenic Ras processing and signaling (Lerner *et al.*, 1995). GGTI-298 has been shown to block PDGF- and epidermal growth factor-dependent tyrosine phosphorylation of their corresponding tyrosine kinase receptors, whereas inhibition of protein farnesylation with FTI-277 has no effect on receptor tyrosine kinase phosphorylation (McGuire *et al.*, 1996). GGTI-298 was found to inhibit the growth of human tumors in nude mice (Sun *et al.*, 1998). The mechanism for this activity may be similar to the GGTI-298-mediated G_1 phase block and subsequent apoptosis in cultured human tumor cells (Miquel *et al.*, 1997). GGTI-298 also induces G_1 arrest and apoptosis in rat pulmonary artery smooth muscle cells. Furthermore, GGTI-298 inhibited the ability of PDGF, interleukin-1beta, and activated Ras to induce superoxide production in smooth muscle cells (Stark *et al.*, 1998). In summary, GGTI-298 has antiproliferative effects on fibroblasts, epithelial, and smooth muscle cells, which appear to be mediated by arrest of G_1 phase (Vogt *et al.*, 1997).

Treatment of human cancer cells, including bladder, lung, colon, brain, and breast cancers, with GGTI-298 and FTI-277 results in increased RhoB expression. Induction of RhoB takes place at the transcriptional level. Actinomycin D was found to prevent this

induction of RhoB. Treatment of cancer cells with GGTI or FTI resulted in the separation of histone deacetylase 1 (HDAC1), binding of histone acetyltransferase (HAT), and resulted in acetylated histones in the promoter region of RhoB. These results show that the level of RhoB expression, in cells treated with GGTI or FTI, is modulated by the acetylation of the RhoB promoter (Delarue *et al.*, 2007).

Regulation of LPA_1R Trafficking

We have been studying the trafficking of the most widely expressed GPCR for the bioactive lipid lysophosphatidic acid (LPA), the LPA_1R. LPA is an abundant serum lysophospholipid that evokes growth factor-like responses through GPCR activation. LPA promotes cell growth and survival (van Corven *et al.*, 1992; Fang *et al.*, 2000; Goetzl *et al.*, 2000), causes cytoskeletal rearrangements (Ridley and Hall, 1992), stimulates serum-responsive genes (Hill *et al.*, 1995), and promotes cancer progression (Hama *et al.*, 2004; Kue *et al.*, 2002; Mills and Moolenaar, 2003; Mukai *et al.*, 2000; Stam *et al.*, 1998; Xu *et al.*, 1995;). LPA activates at least five distinct GPCRs, which collectively can activate G_s, G_i, $\beta\gamma$, G_q, and $G_{12/13}$ signaling pathways (Meyer zu Heringdorf and Jakobs, 2007). LPA_1Rs are internalized in response to LPA stimulation through a pathway that depends on clathrin and β-arrestin (Wang *et al.*, 2001; Murph *et al.*, 2003; Urs *et al.*, 2005). However, unlike other GPCRs, LPA_1Rs require membrane cholesterol to associate with β-arrestins (Urs *et al.*, 2005). Once internalized, LPA_1Rs transit through early endosomes and localize to recycling endosomes, wherein they extensively colocalize with transferrin receptors (Murph *et al.*, 2003). The removal of LPA results in a rapid recycling of LPA_1Rs from recycling endosomes back to the plasma membrane. Our present results from studying the effects of statins and prenylation

inhibitors on the membrane trafficking of the LPA_1Rs implicate RhoC and RhoA, in the regulation of LPA_1R recycling from endosomes through a mechanism that is distinct from that utilized by transferrin receptor recycling pathway. The results of these studies will be described in detail below.

CHAPTER 2

MATERIALS AND METHODS

Antibodies and reagents

Lysophosphatidic acid (1-oleoyl-2-hydroxy-*sn*-glycero-3-phosphate; LPA) was purchased from Avanti Polar Lipids (Alabaster, AL). FLAG-tagged LPA_1R receptors were detected with mouse anti-M1 FLAG or rabbit anti-FLAG antibodies (Sigma Chemical Co., St. Louis, MO). HA-tagged β_2ARs and HA-tagged LPA_1Rs were detected with mouse anti-HA antibodies (Covance, Berkeley, CA). Anti-transferrin receptor mouse monoclonal antibody (clone B3/25) was from Boehringer Mannheim (Mannheim, Germany). The mouse anti-LAMP-1 antibody was obtained from the Developmental Studies Hybridoma Bank developed under the auspices of the NICHD and maintained by The University of Iowa, Department of Biological Sciences (Iowa City, IA). Anti-EEA1 was from BD Biosciences (San Jose, CA). Rat monoclonal antibody against human M_2 mAChRs was obtained from Chemicon, Inc. (Temecula, CA). Cy2- and Cy3-conjugated goat anti-mouse IgG, goat anti-rabbit IgG, goat anti-rat IgG, anti-human golgin-97 mouse monoclonal antibody, and Hoechst 33342 were purchased from Molecular Probes, Inc (Eugene, OR). Atorvastatin calcium was obtained from JMar Chemical Co. (Englewood, CO), prepared as a 10 mM solution in DMSO, and stored at -80 °C. Mevastatin was purchased from Tocris (Ellisville, MO) and was prepared as a 10 mM solution in DMSO and stored at -80 °C. Geranylgeranyltransferase inhibitor (GGTI-298) and farnesyltransferase inhibitor (FTI-277) were from Calbiochem (La Jolla, CA). These compounds were prepared as 20 mM solutions in DMSO and stored at -80 °C. Farnesylpyrophosphate (FPP), geranylgeranylpyrophosphate (GGPP), and ubiquinone

from Sigma Chemical Co. were dissolved in methanol and stored at -20 °C. *Myo*-[^{3}H] inositol was purchased from American Radiolabeled Chemicals, Inc. (St. Louis, MO). All other reagents were obtained from Sigma Chemical Co., unless otherwise specified.

Cell culture and DNA transfection

LPA_1R/HeLa cells, which stably-express FLAG-tagged or HA-tagged human LPA_1R, and HeLa cells were maintained in Dulbecco's modified Eagle's medium (DMEM) supplemented with 10% fetal bovine serum, 100 I.U./ml penicillin, 100 µg/ml streptomycin (Media Tech, Inc, Herndon, VA), and 1mM sodium pyruvate (Biosource International, Camarillo, CA) at 37 °C with 5% CO_2. Cells were grown on glass coverslips (for immunolocalization) and transfected in six-well dishes, or were grown in 24-well dishes for *myo*-[^{3}H] inositol labeling. Transient transfections were performed using ExGen 500 (Fermentas Inc., Hanover, MD), according to the manufacturer's directions. Plasmids encoding M_2 mAChRs were transiently transfected into LPA_1R/HeLa cells at one µg/well (6-well dish). Plasmids encoding HA-tagged β_2AR were transfected at 1 µg/well (6-well dish) (Kim and Benovic, 2002; Paing *et al.*, 2002). Cells were incubated in serum free DMEM supplemented with 1mM sodium pyruvate (SFM) for 24 prior to immunolocalization. All drug treatments were performed in SFM with the medium and treatments refreshed every 24 h. For transient transfection experiments, statins and prenylation inhibitors were present from the start of transfection.

Indirect immunofluorescence

Cells were treated as described in the figure legends, 24-48 h after transfection. Cells were then fixed in 2% formaldehyde in phosphate buffered saline (PBS) for 10 min., and rinsed with 10% fetal bovine serum (FBS) containing 0.02% azide in PBS

(PBS-serum). Fixed cells were incubated with primary antibodies diluted in PBS-serum containing 0.2% saponin for 1 h, and then washed (3 times, 5 min each) with PBS-serum. The cells were then incubated with fluorescently labeled secondary antibodies diluted in PBS-serum containing 0.2% saponin for 1 h, washed three times with PBS-serum, washed once with PBS, and mounted on glass slides as previously described (Murph *et al.*, 2003). All images were acquired using an Olympus BX40 epifluorescence microscope equipped with a 60x Plan pro lens and photomicrographs were prepared using an Olympus MagnaFire SP digital camera (Olympus America Inc., Melville, NY). Images were processed using Adobe Photoshop 6.0 (Adobe Systems Inc., San Jose, CA).

Quantification of LPA_1R colocalization with TfnR

LPA_1R/HeLa cells were grown on glass coverslips and treated as described in the figure legends. The cells were then rinsed with PBS, fixed with 2% formaldehyde in PBS, and processed for immunofluorescence localization of LPA_1R using rabbit anti-FLAG and TfnR using mouse anti-TfnR, followed by Cy2- and Cy3- conjugated secondary antibodies. The extent of LPA_1R colocalization with TfnR was determined by quantifying the extent of pixel colocalization of LPA_1R staining with TfnR fluorescence using Metamorph Imaging software (Urs *et al.*, 2005). The background was subtracted from unprocessed images and the percentage of LPA_1R pixels that overlapped with TfnR pixels was measured. The data presented is the mean ± s.e.m. of the indicated number of cells per sample obtained from a representative experiment that was performed three independent times with similar results.

Antibody internalization assay

HeLa cells stably expressing HA-tagged LPA_1Rs were either pretreated with vehicle (DMSO) or with atorvastatin (10 μM) for 24 h, chilled to 4°C, and incubated for 30 min with 2.5 μg/ml anti-HA antibodies diluted in serum-free medium. Excess antibodies were removed by washing with serum-free medium. For untreated cells and cells pre-treated with atorvastatin, these samples were warmed to 37°C in the presence of atorvastatin (10 μM) for an additional 24 hr. For GGTI-298-treated samples, these cells were warmed to 37°C for 4 hours with 20 μM GGTI-298. Following treatments at 37°C, antibodies bound to the cell surface were removed by rinsing the cells with 100 mM glycine, 20 mM magnesium acetate, 50 mM KCl, pH 2.2 (acid wash) (Naslavsky *et al.*, 2004b) for 90 seconds, while retaining internalized antibody. The cells were then fixed in 2% formaldehyde in PBS and mounted on glass slides. Images were taken using a Hamamatsu digital camera mounted on a Leica Inverted microscope with a 63X oil immersion objective. The images were analyzed by Simple PCI software (Compix, Cranberry Township, PA) and total fluorescence (vesicles/cell) for both internalized and surface antibody levels were measured as described previously (Xiao *et al.*, 2005). Internalization (fluorescence after acid wash) is expressed as a percentage of total fluorescence of initial surface bound antibodies (4°C).

Transferrin recycling

LPA_1R/HeLa cells were plated on glass coverslips and treated as indicated. Following treatment, cells were loaded with Alexa 546-transferrin (20 μg/mL) (generously provided by Dr. Fred Maxfield (Weill Medical College of Cornell

University, New York, NY)) for 30 min. at 37 °C. Loading was terminated with two washes in mild acid buffer (50 mM 2-(*N*-morpholino)ethanesulfonic acid, 280 mM sucrose, pH 5.0, 37 °C), and four washes in SFM (Presley *et al.*, 1993). The cells were then incubated at 37 °C in chase medium (SFM containing 0.5 mg/mL unlabeled Tfn and 20 μM desferroxamine) for various periods. Following the chase, cells were washed twice in mild acid buffer, washed four times with SFM, and fixed in 2% formaldehyde in PBS for 10 min. Cells were then washed once with PBS and mounted on glass slides. Integrated fluorescence intensity per cell was quantified using Metamorph Imaging software (Universal Imaging, West Chester, PA).

Phosphoinositide hydrolysis

LPA_1R/HeLa cells were plated at a density of 4.0×10^4 cells/well into 24-well plates. At 24 h post-transfection, cells were labeled overnight with *myo*-[^{3}H] inositol in inositol- and serum-free medium, treated as described in the figure legends, and then processed for analysis of phosphoinositide hydrolysis by anion exchange chromatography, as described (Paing *et al.*, 2002; Urs *et al.*, 2005).

Membrane and cytosol fractionation

LPA_1R/HeLa cells were grown in 10 cm dishes. Following treatment, cells were rinsed twice with ice cold PBS on ice/water bath. Cells were then scraped into 4 mL of ice cold PBS. Cells were pelleted for 5 min. at 300×g at 4 °C, resuspended in 1 mL of 250 mM sucrose, 10 mM Tris-Cl (pH 7.4), and pelleted again for 5 min. at 300×g at 4 °C. Cells were resuspended in 0.5 mL of 100 mM sucrose, 10 mM Tris-Cl (pH 7.4), and then broken by passing the suspension through a 25 gauge syringe needle 15 times. The

suspension was then centrifuged for 10 min. at 800×g at 4 °C (Song *et al.*, 1998). Postnuclear supernatant (PNS) was then transferred to a chilled tube and protein content was determined by BCA Protein Assay. Exactly 50 µg of PNS from each sample was centrifuged for 30 min. at 100,000×g at 4 °C . The supernatant was removed and mixed with an appropriate volume of 4× SDS sample buffer. The pellet was solubilized in an equal volume of 1× SDS sample buffer. Samples were incubated for 5 min. at 95 °C prior to separation of equal volumes by SDS-PAGE and immunoblotting.

Immunoblotting

Following treatment, cells were solubilized by addition of lysis buffer (1% NP-40, 1% sodium deoxycholate, 0.1% SDS, 0.15 M NaCl, 0.01 M sodium phosphate pH 7.2, 2 mM EDTA, 50 mM NaF, 0.2 M sodium orthovanadate, 0.02% azide, 100 µg/ml leupeptin and 0.1 mM PMSF) . The samples (12 µg protein per lane) were then separated by 10% SDS-PAGE and transferred to nitrocellulose. Detection of HRP-conjugated secondary antibodies was performed with SuperSignal West Pico Chemiluminescent Substrate (Pierce Biotechnology), followed by exposure to Kodak BioMax Light Film. Films were scanned on a flatbed scanner and bands were quantified using Metamorph Imaging software.

RNA interference

Cells were transfected using Lipofectamine™ RNAiMAX Reagent in Opti-MEM® I Reduced Serum Medium (Invitrogen, Carlsbad, CA). Stealth™ Select 3 RNAi Sets directed against RhoA, RhoB, or RhoC (Table 1) were used as instructed by the manufacturer (Invitrogen). The cells were transfected a second time, as above, and the

medium was then replaced with SFM and incubated for an additional 24 hours before experimentation. Medium GC Stealth™ RNAi Negative Control Duplexes (Cat. # 12935-300) were used as instructed by the manufacturer (Invitrogen). Transfection efficiency of over 80% was confirmed by cotransfection of cells with BLOCK-iT™ Fluorescent Oligo (Invitrogen).

Table 1: Sequences of siRNAs directed against RhoA, RhoB, or RhoC.

	Sequence
siRhoA 1 Sense	GCCUGUGGAAAGACAUGCUUGCUCA
siRhoA 1 Antisense	UGAGCAAGCAUGUCUUUCCACAGGC
siRhoA 2 Sense	ACCCAGAUACCGAUGUUAUACUGAU
siRhoA 2 Antisense	AUCAGUAUAACAUCGGUAUCUGGGU
siRhoA 3 Sense	CAGCAAAGACCAAAGAUGGAGUGAG
siRhoA 3 Antisense	CUCACUCCAUCUUUGGUCUUUGCUG
siRhoB 1 Sense	CGUGCCUGCUGAUCGUGUUCAGUAA
siRhoB 1 Antisense	UUACUGAACACGAUCAGCAGGCACG
siRhoB 2 Sense	GUCUUCGAGAACUAUGUGGCCGACA
siRhoB 2 Antisense	UGUCGGCCACAUAGUUCUCGAAGAC
siRhoB 3 Sense	ACACCGACGUCAUUCUCAUGUGCUU
siRhoB 3 Antisense	AAGCACAUGAGAAUGACGUCGGUGU
siRhoC 1 Sense	GCAAGGAUCAGUUUCCGGAGGUCUA
siRhoC 1 Antisense	UAGACCUCCGGAAACUGAUCCUUGC
siRhoC 2 Sense	CCCUACUGUCUUUGAGAACUAUAUU
siRhoC 2 Antisense	AAUAUAGUUCUCAAAGACAGUAGGG
siRhoC 3 Sense	GGAUCAGUGCCUUUGGCUACCUUGA
siRhoC 3 Antisense	UCAAGGUAGCCAAAGGCACUGAUCC

RT-PCR

Total RNA was isolated from the cells using RNeasy® Plus Mini Kit columns (QIAGEN, Valencia, CA). Primers targeting RhoA (sense, 5'-CTGGTGATTGTTGGTGATGG-3'; antisense, 5'-GCGATCATAATCTTCCTGCC-3'; spanning 183 bp), RhoB (sense, 5'-TGCTGATCGTGTTCAGTAAG-3'; antisense, 5'-AGCACATGAGAATGACGTCG-3'; spanning 189 bp), or RhoC (sense, 5'-TCCTCATCGTCTTCAGCAAG-3'; antisense, 5'-GAGGATGACATCAGTGTCCG-3'; spanning 181 bp) were ordered from Integrated DNA Technologies, Inc. (Coralville, IA). RT-PCR was performed using a QIAGEN OneStep RT-PCR Kit, as instructed by the manufacturer. A QuantumRNA™ 18S Internal Standards Kit (Ambion, Austin, TX) was used as a standard control, as instructed by the manufacturer. Reverse transcription was conducted at 50 °C for 30 min., followed by 15 min. at 95 °C, to deactivate reverse transcriptase. The cDNA fragments were then denatured at 94 °C for 30 sec., annealed at 58 °C for 1 min., and extended at 72 °C for 1 min. After 30 cycles of amplification, followed by a final extension at 72 °C for 10 min., the PCR products were analyzed on a 2% agarose gel and the bands were visualized using ethidium bromide during exposure to a UV transilluminator.

Statistical analysis

The data is expressed as the mean ± s.e.m. from the indicated number of independent experiments performed in triplicate. Differences were analyzed by two-factor ANOVA followed by a Tukey's statistical significance test.

CHAPTER 3

RESULTS

Inhibition of protein geranylgeranylation induces the sequestration of cell surface LPA1Rs, but not transferrin receptors, in recycling endosomes

We have previously shown that the clathrin- and β-arrestin-dependent internalization of LPA_1R requires membrane cholesterol, since acute cholesterol extraction prevents β-arrestin association and blocks LPA_1R endocytosis (Murph *et al.*, 2003; Urs *et al.*, 2005). To further study this, we examined the effects of the HMG-CoA reductase inhibitors atorvastatin and mevastatin on the localization of LPA_1R, stably expressed in HeLa cells (Figure 2A). Treatment of cells with 10 μM atorvastatin for up to 24 h neither altered the diffuse plasma membrane localization of LPA_1R observed in control, vehicle-treated cells, nor did it inhibit LPA-induced internalization of LPA_1R into endosomes (Figure 2A, 24 h 10 μM LPA). In contrast, incubation of cells with atorvastatin for 48 h induced the localization of LPA_1R into endosomal structures even in the absence of exogenously added LPA, and subsequent addition of LPA (10 μM) did not further enhance this endosomal localization. Atorvastatin did not alter cell viability over this 48 h treatment time (data not shown). Treatment with another HMG-CoA reductase inhibitor, mevastatin (10 μM), also induced an endosomal localization of LPA_1R, indicating that this effect was not unique to atorvastatin.

We have previously shown that LPA_1R localizes to transferrin receptor$^+$ recycling endosomes following agonist stimulation (Murph *et al.*, 2003). Double-label immunofluorescence labeling experiments showed that LPA_1R co-localized with both

transferrin receptors and co-expressed Rab11-GFP following atorvastatin-induced sequestration (Figure 2B). In contrast, LPA_1R showed little co-localization with the early endosomal marker, EEA1 (data not shown). This suggested that statin treatment led to sequestration of LPA_1R in juxtanuclear recycling endosomes. To assess effects of this altered distribution of LPA_1Rs on signaling, we examined the effects of atorvastatin (1 μM) on the kinetics of LPA stimulation of phosphoinositide (PI) hydrolysis, which is mediated by $G\alpha_q$ and phospholipase C (Urs *et al.*, 2005). Whereas atorvastatin did not alter the EC_{50} of LPA-induced PI hydrolysis (EC_{50} = 1.939 μM, control and atorvastatin-treated cells), it did reduce the rate and maximal extent of PI hydrolysis (Figure 2C).

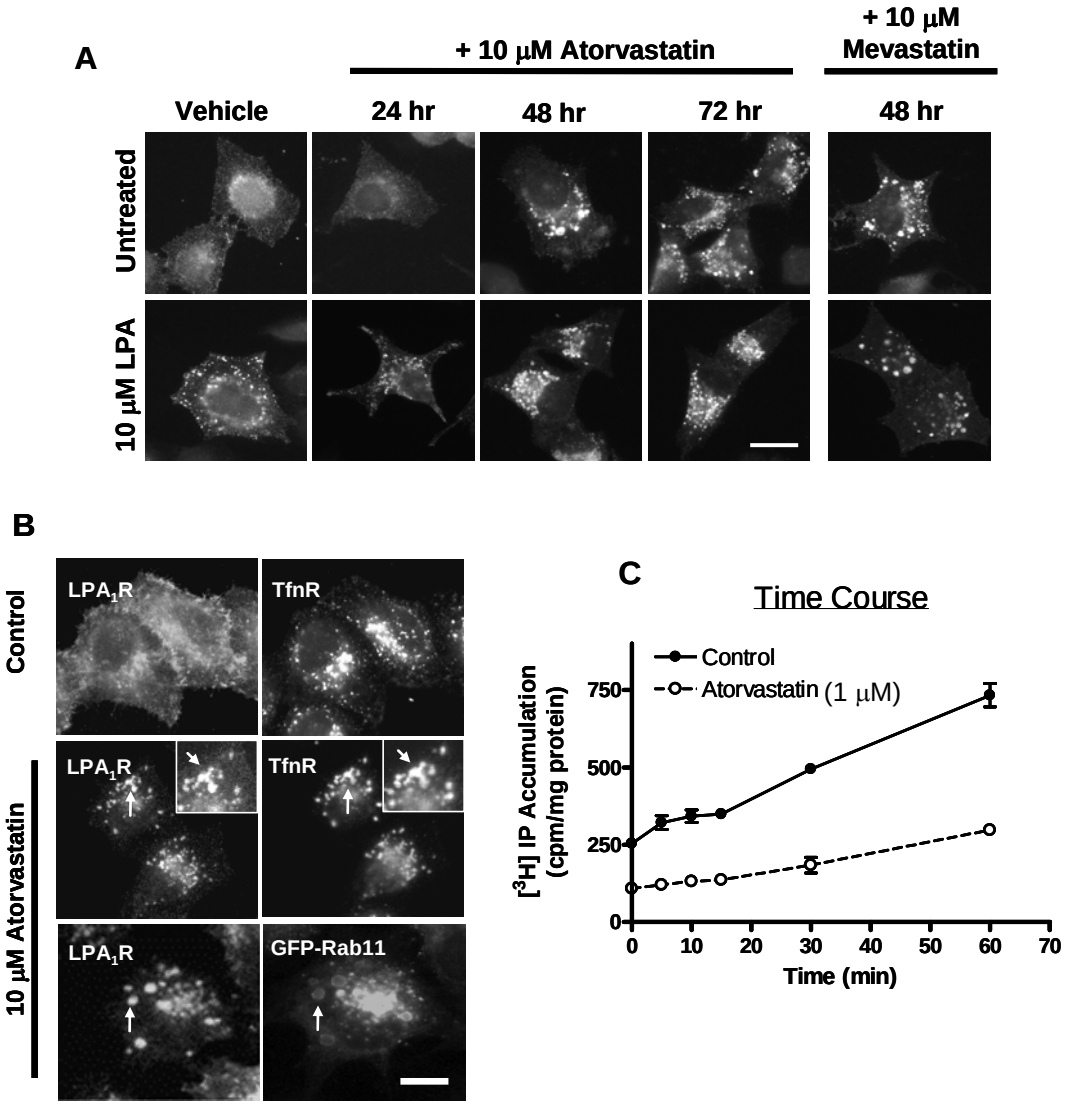

Figure 2: Statins induce endosomal sequestration of LPA_1Rs and reduce LPA signaling efficiency.

(A) Atorvastatin (10 μM) and Mevastatin (10 μM) induce a redistribution of LPA_1R receptors to punctate endosomal structures in a time-dependent manner independently of agonist stimulation as observed immunofluorescence microscopy. Vehicle is 48 h treatment with DMSO. Bar, 10 μm. **(B)** Atorvastatin (10 μM for 48 h) induces the redistribution of LPA_1Rs into $TfnR^+$ and $Rab11^+$ recycling endosomes. Arrows indicate endosomes where LPA_1R colocalizes with TfnR or GFP-Rab11. The inset is a higher magnification of endosomal structures that are positive for both LPA_1R and TfnR. Bar, 10 μm. **(C)** Pretreatment with atorvastatin (1 μM for 48 h) reduces the kinetics and extent of LPA-dependent phosphoinositide hydrolysis; cells were stimulated with 1 μM LPA for up to 60 min. Values represent the means ± s.e.m. of triplicate measurements obtained from a representative experiment that was repeated three times with similar results.

In addition to reducing endogenous cholesterol production, statins also deplete isoprenoid lipids, which are involved in protein prenylation (Figure 3) (Leung *et al.*, 2006). Since we have shown that acute cholesterol depletion inhibits LPA_1R internalization (Urs *et al.*, 2005) rather than induce internalization, we hypothesized that atorvastatin-induced endosomal sequestration might be due to its affects on isoprenoid abundance. To test this, we compared the effects of combining atorvastatin (1 μM) with different isoprenoids on the localization of LPA_1R (Figure 4A). We hypothesized that adding back the relevant downstream lipid product would prevent atorvastatin-induced endosomal sequestration and thus, reduce the colocalization of LPA_1Rs with TfnR. LPA_1R localized to $TfnR^+$ endosomes in cells treated with atorvastatin alone and in cells treated with atorvastatin plus either farnesylpyrophosphate (FPP) (10 μM) or ubiquinone (50 μM); indicating that these lipid products do not rescue the atorvastatin-induced endosomal sequestration of LPA_1Rs. In contrast, LPA_1Rs remained at the cell surface, like control untreated cells, when treated with atorvastatin and geranylgeranylpyrophosphate (GGPP) (1 μM); indicating that this lipid prevents atorvastatin-induced endosomal sequestration of LPA_1Rs. Quantification of the percentage of cells exhibiting LPA_1R co-localization with TfnR (e.g., a measure of endosomal sequestration) indicated that co-addition of either geranylgeranylpyrophosphate (GGPP) (1 μM) or geranylgeraniol (GGOH) (1 μM) markedly reduced atorvastatin-induced endosomal sequestration of LPA_1Rs; neither farnesylpyrophosphate (FPP) (1 μM or 10 μM) nor farnesol (FOH) (1 μM or 10 μM) was able to inhibit atorvastatin-induced endosomal sequestration (Figure 4B). These results suggested that atorvastatin-dependent depletion of geranylgeranylpyrophosphate was

responsible for the endosomal sequestration of LPA_1R and that defects in protein geranylgeranylation of some relevant target was the primary cause.

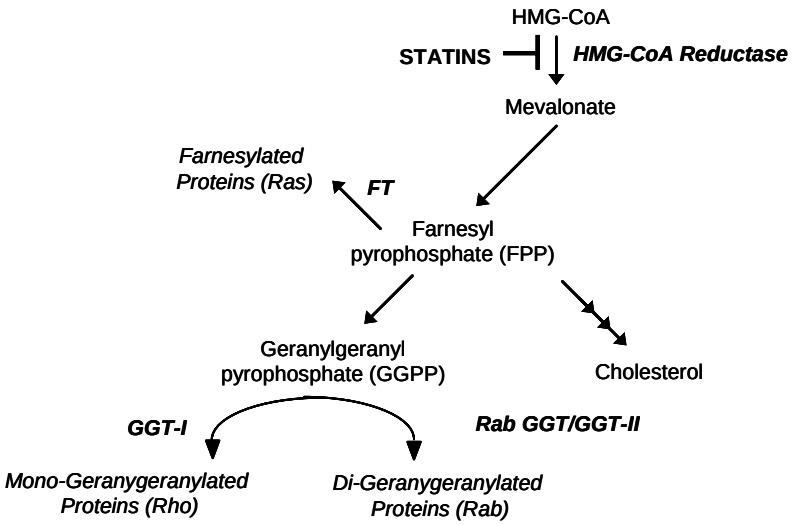

Figure 3: HMG-CoA reductase pathway.
Diagram of the HMG-CoA reductase pathway leading to isoprenoid synthesis and protein prenylation.

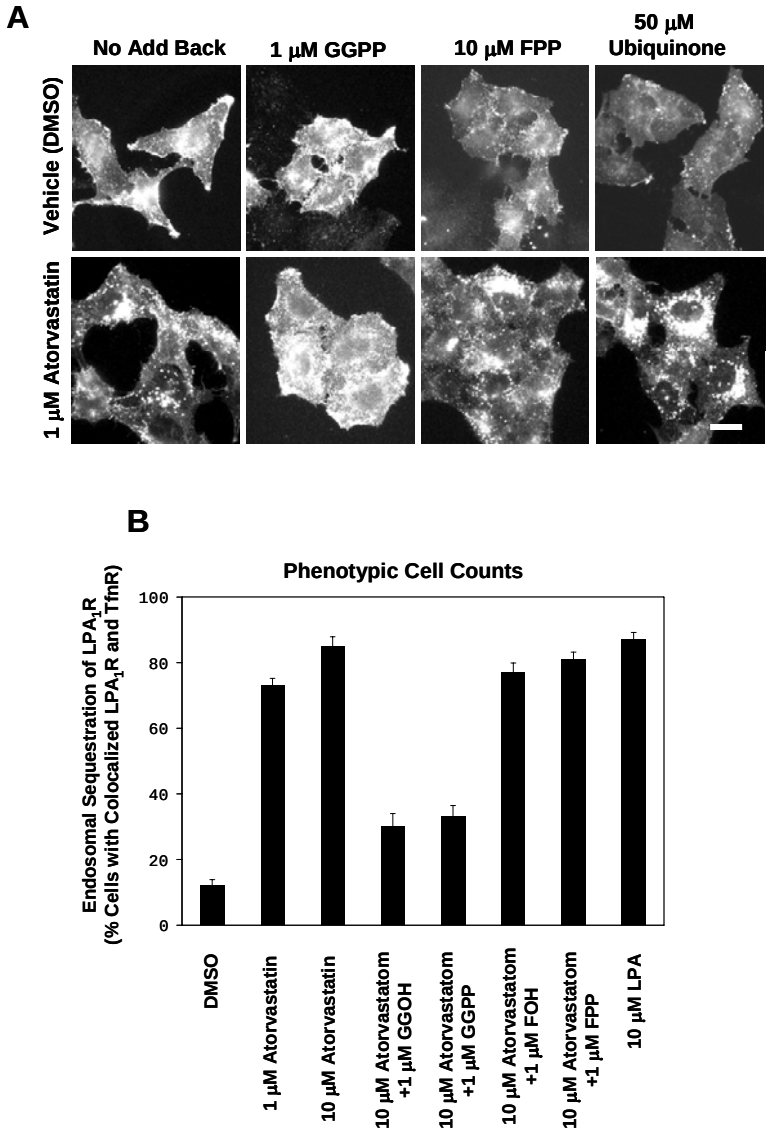

Figure 4: Co-addition of the down-stream HMG-CoA reductase product, GGPP, prevents atorvastatin-induced sequestration of LPA_1Rs in recycling endosomes.
(A) Addition of GGPP (1 μM), but not FPP (10 μM) or ubiquinone (50 μM) prevents atorvastatin-induced endosomal sequestration of LPA_1R. Bar, 10 μm. **(B)** Phenotypic quantification shows that both GGOH and GGPP reduce the atorvastatin-induced redistribution of LPA_1R into $TfnR^+$ recycling endosomes. Cells were treated with the indicated compounds for 48 h, fixed, and processed for immunofluorescence localization of LPA_1Rs and TfnRs. Values are the means ± s.e.m. of quadruplicate samples (n=100 cells/condition) from a representative experiment that was repeated three times with similar results.

To test this hypothesis directly, we examined the effects of specific inhibitors of geranylgeranyltransferase-1 (GGTI-298) (McGuire *et al.*, 1996) and farnesyltransferase (FTI-277) (Lerner *et al.*, 1995) on the localization of LPA_1Rs (Figure 5A). Treatment with GGTI-298 for 24 h led to a marked colocalization of LPA_1Rs with transferrin receptors in endosomes. This increased endosomal localization of LPA_1Rs could be observed after only 1 h of GGTI treatment (Figure 5A, bottom panels). In contrast, vehicle-treated cells and cells treated with FTI-277 showed a diffuse cell surface localization for LPA_1R with little colocalization with transferrin receptors. These data indicate that inhibition of protein geranylgeranylation either through depletion of isoprenoids with atorvastatin or through direct inhibition of geranylgeranyltransferase-1 with GGTI-298 induced marked redistribution of LPA_1Rs to recycling endosomes.

Previous studies have shown that agonist stimulation induces the internalization of surface LPA_1Rs into endosomes (Wang *et al.*, 2001; Murph *et al.*, 2003; Urs *et al.*, 2005). We next quantified the effects of atorvastatin, GGTI-298, and FTI-277 on the extent of LPA_1R sequestration in recycling endosomes by using image analysis to measure the co-localization of LPA_1Rs and transferrin receptors (Figure 5B). As expected, agonist stimulation with LPA (10 μM) greatly enhanced colocalization of LPA_1Rs and TfnRs to approximately 80% per cell. Atorvastatin (10 μM, 48 h) and GGTI-298 (20 μM, 24 h) also enhanced the colocalization of LPA_1Rs and TfnRs to 85% and 78% per cell, respectively. In contrast, FTI-277 (20 μM, 24 h) did not promote the colocalization of LPA_1Rs and TfnRs in recycling endosomes (only 24% fluorescence overlap).

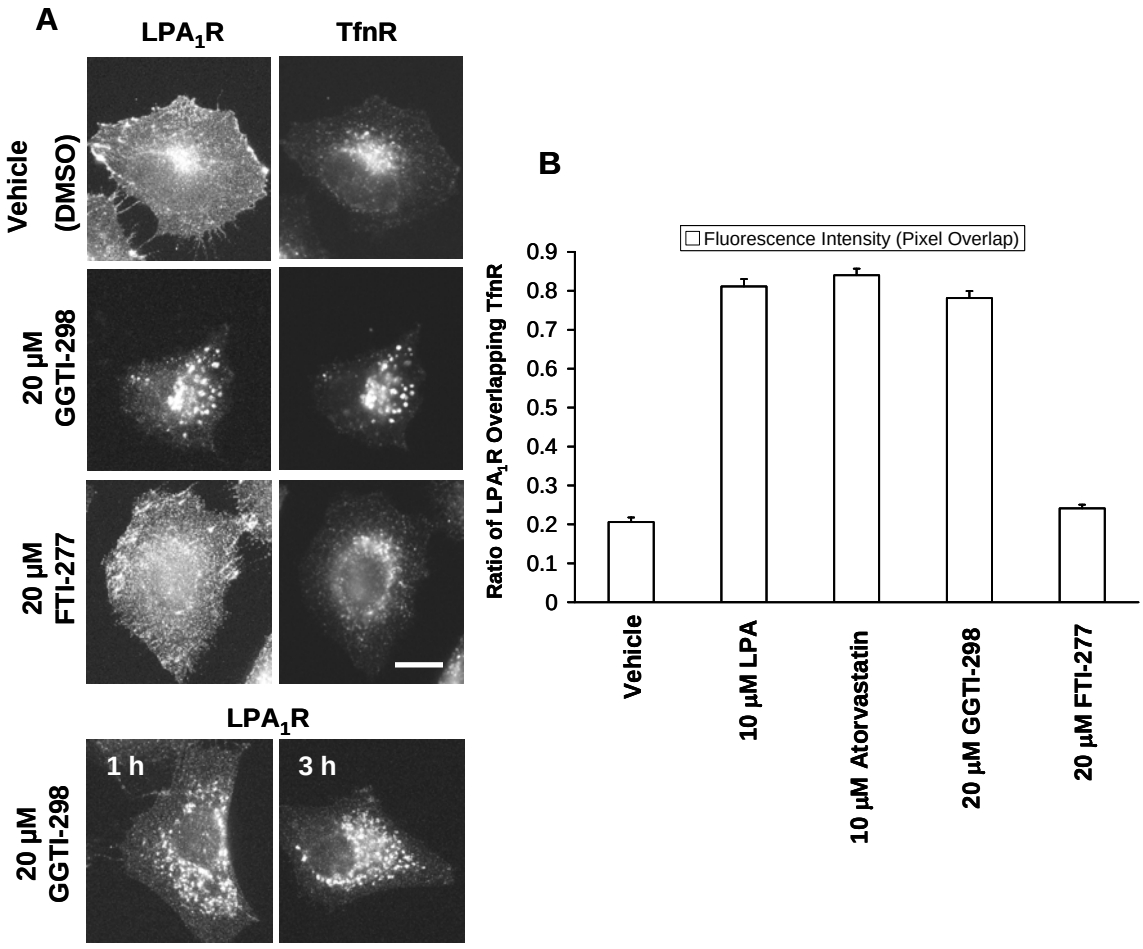

Figure 5: Atorvastatin and GGTI induce the sequestration of LPA_1Rs.
(A) Treatment with the geranylgeranyltransferase-I inhibitor, GGTI-298, for 24 h induces the localization of LPA_1Rs to $TfnR^+$ endosomes (upper panel); localization of LPA_1Rs to endosomes was observed as quickly as after 1 h of treatment with GGTI-298 (lower panels). The farnesyltransferase inhibitor, FTI-277 (20 μM, 24 h), did not induce endosomal localization of LPA_1Rs. Bar, 10 μm. **(B)** LPA, atorvastatin, and GGTI-298 increase the colocalization of LPA_1Rs and TfnRs in recycling endosomes as determined by immunofluorescence microscopy and quantification of fluorescence overlap between the two proteins. The data are the mean ± s.e.m. of the extent of fluorescence overlap; 15 cells per condition were analyzed and the data are from a representative experiment, which was repeated at least three times with similar results.

To further investigate whether the LPA_1Rs that accumulate in endosomes are internalized from the cell surface, we took advantage of the fact that the N-terminal epitope tag (either FLAG or HA) that is present on the LPA_1Rs is able to bind and internalize anti-epitope antibodies added to the culture medium. We incubated HeLa cells that stably expressed HA-tagged LPA_1Rs (for these experiments) with anti-HA antibodies in the presence or absence of atorvastatin (10 μM, 48 h) and then quantified the proportion of bound antibodies that were internalized into cells by image analysis (Figure 6). Whereas only 6 ± 0.6% of the initially bound anti-HA antibodies were internalized and retained in untreated cells, 89 ± 3.2% of the initially bound anti-HA antibodies were internalized in cells treated with atorvastatin; thus, strengthening the hypothesis that the LPA_1Rs that are sequestered in endosomes are derived from the cell surface. Similarly, incubation of cells with anti-HA antibodies and GGTI-298 (20 μM, 24 h) led to the internalization and retention of 71 ± 3% of the initially bound anti-HA antibodies. Taken together, these results strongly suggested that inhibition of protein geranylgeranylation by atorvastatin or GGTI-298 induces the endosomal sequestration of cell surface LPA_1Rs.

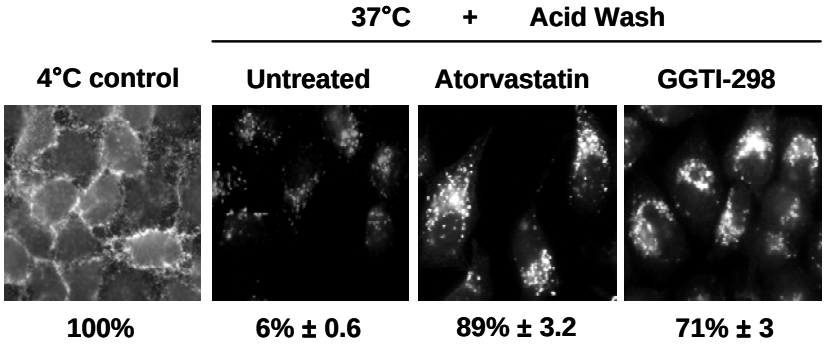

Figure 6: Atorvastatin and GGTI induce the sequestration of cell surface LPA_1Rs. Atorvastatin (10 μM, 48 h) and GGTI-298 (20 μM, 24 h) induce the endosomal retention of internalized anti-epitope antibodies, which were initially bound to cell surface LPA_1Rs at 4°C. The untreated condition was incubated at 37°C for 48 h. Following treatment with the inhibitors, the remaining surface antibodies were removed with an acid wash prior to fixation and analysis by immunofluorescence microscopy. The data from fluorescence quantification of the internalized anti-epitope antibodies are shown below each micrograph; the data were normalized to the fluorescence intensity of antibodies initially bound at 4°C (see methods for more details).

To determine whether atorvastatin induced the endosomal sequestration of other GPCRs, we transiently expressed HA-tagged versions of either β_2-adrenergic receptors (β_2ARs) or M_2 muscarinic acetylcholine receptors (M_2 mAChRs) in HeLa cells, which stably expressed FLAG-tagged LPA_1R. In cells treated with vehicle alone, LPA_1R, β_2ARs, and M_2 mAChRs were predominantly localized at the cell surface and in the perinuclear region of cells (Figure 7 vehicle-treated panels); this latter compartment readily labeled with antibodies to the Golgi complex marker, Golgin-97, suggesting that these were newly synthesized receptors en route to the cell surface (data not shown). After treatment with atorvastatin (10 μM) for 48 h, all three receptors were co-localized in recycling endosomes (Figure 7). This suggested that atorvastatin induces the endosomal sequestration of other GPCRs, in addition to LPA_1Rs. Both β_2ARs and M_2 mAChRs undergo agonist-induced endocytosis, with β_2ARs utilizing a β-arrestin and clathrin-dependent pathway (Urs *et al.*, 2005).

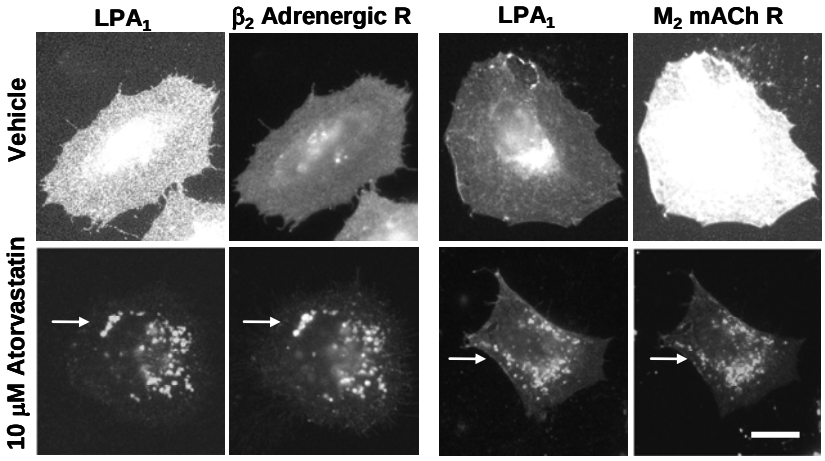

Figure 7: Statin treatment induces the sequestration of multiple GPCRs in recycling endosomes.

β_2-ARs and M_2 mAChRs are sequestered in recycling endosomes with LPA_1Rs following atorvastatin treatment (10 μM for 48 h) as observed by immunofluorescence microscopy; HA-tagged β_2ARs or HA-tagged M_2 mAChRs were expressed in HeLa cells that stably expressed FLAG-tagged LPA_1Rs. Arrows indicate endosomes where LPA_1R colocalizes with β_2ARs or M_2 mAChRs. Bar, 10 μm.

Whereas most GPCRs undergo conditional, agonist-stimulated internalization, transferrin receptors are constitutively internalized and recycled from endosomes. We examined the effects of atorvastatin, GGTI-298, and FTI-277 on both the internalization and recycling of Alexa 546-labeled transferrin (Alexa-Tfn), using image analysis to quantify cell-associated Alexa-Tfn. HeLa cells stably-expressing LPA_1Rs were incubated with vehicle (DMSO), atorvastatin (10 μM, 48 h), GGTI-298 (20 μM, 24 h), or FTI-277 (20 μM, 24 h) prior to incubation with Alexa-Tfn for 30 min. Both vehicle-treated and atorvastatin-treated cells internalized Alexa-Tfn into small punctate endocytic structures as well as larger juxtanuclear endosomes (Figure 8A). Image analysis showed that cells treated with vehicle, atorvastatin, GGTI-298, and FTI-277 all contained nearly the same amount of Alexa-Tfn (Figure 8B, white bars). This indicated that treatment of cells with atorvastatin, GGTI-298, or FTI-277 did not alter transferrin receptor endocytosis. To assess recycling of transferrin from endosomes, cells that were loaded for 30 min with Alexa-Tfn were chased with medium containing the iron chelator, desferroxamine, and excess unlabelled transferrin for 2 h. Immunofluorescence images showed a significant reduction in cell-associated Alexa-Tfn (Figure 8A); fluorescence quantification (Figure 8B, black bars) indicated that approximately 60% of the internalized Alexa-Tfn was lost from the cells, regardless of the inhibitors used. This indicated that atorvastatin, GGTI-298, and FTI-277 do not inhibit transferrin receptor endocytosis or recycling.

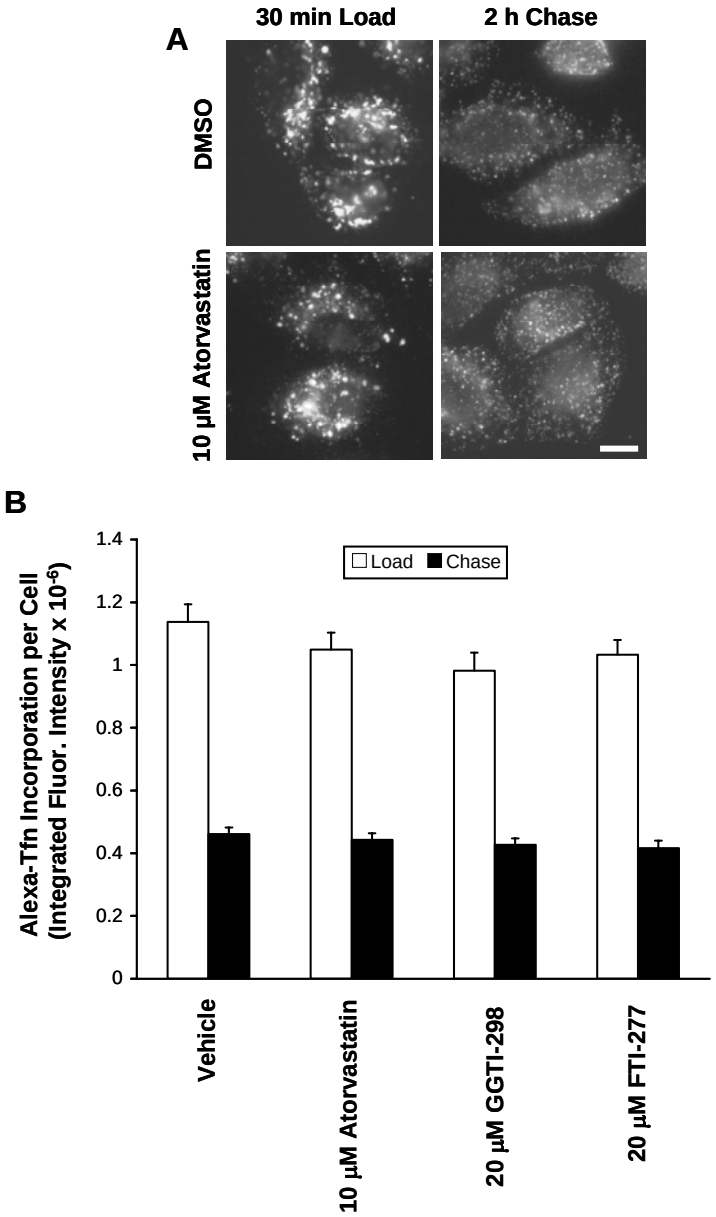

Figure 8: Neither atorvastatin nor incubation with prenylation inhibitors alter the internalization or recycling of Alexa-transferrin.

(A) Atorvastatin treatment (10 µM for 48 h) perturbs neither the internalization of Alexa 546-Tfn into recycling endosomes nor recycling of Alexa-Tfn during a 2 h washout. **(B)** Fluorescence image quantification showed that none of the inhibitors (atorvastatin, GGTI-298, and FTI-277) inhibited Alexa-Tfn internalization during a 30 min incubation (Load, white bars) and had no affect on Alexa-Tfn recycling out of cells (Chase, black bars); cells were chased for 2 h in medium containing excess unlabeled Tfn and the iron chelator, desferroxamine (see methods). Values are means ± s.e.m. of the fluorescence intensity, which was obtained by quantifying fluorescence intensity of 15 cells per condition from a representative experiment that was repeated three times with similar results.

Atorvastatin and GGTI-298 reduce the cellular abundance of RhoA-related GTPases but do not affect Rab11

A variety of small GTPases, including members of the Rho and Rab family of GTPases, undergo geranylgeranylation, which permits them to associate with membranes. Since LPA_1R accumulates in $TfnR^+$ recycling endosomes following treatment with atorvastatin or GGTI-298, we hypothesized that small GTPases associated with this compartment are the likely targets of inhibition. The Rab11 GTPase is known to localize to recycling endosomes and to regulate recycling of TfnRs (Ullrich *et al.*, 1996). We tested the effects of atorvastatin and GGTI-298 on the partitioning of endogenous Rab11 between soluble and particulate cell fractions (Figure 9A). In control cells, all of the endogenous Rab11 was associated with the particulate fraction. Neither treatment with atorvastatin (10 μM) nor GGTI-298 (20 μM) disrupted the association of Rab11 with particulate cell fractions. These inhibitors also did not alter the cellular abundance of endogenous Rab11. This suggested that Rab11 was not the target of atorvastatin or GGTI-298, which leads to endosomal sequestration of LPA_1Rs. To test whether inhibition of Rab11 would induce endosomal sequestration, we overexpressed either wild type Rab11-GFP or the dominant inhibitory mutant, Rab11-GFP S34N, which inhibits receptor recycling (Ullrich *et al.*, 1996). Neither overexpression of wild type Rab11-GFP nor Rab11-GFP S34N induced the endosomal sequestration of LPA_1R, which was predominantly localized to the plasma membrane (Figure 9B, left panels). Whereas wild type Rab11-GFP localized to large perinuclear endosomal structures, Rab11-GFP S34N showed a diffuse cytoplasmic localization (Figure 9B, right panels).

These results suggested that atorvastatin and GGTI-298 induced endosomal sequestration of LPA_1R is most likely not due to inhibition of Rab11 function.

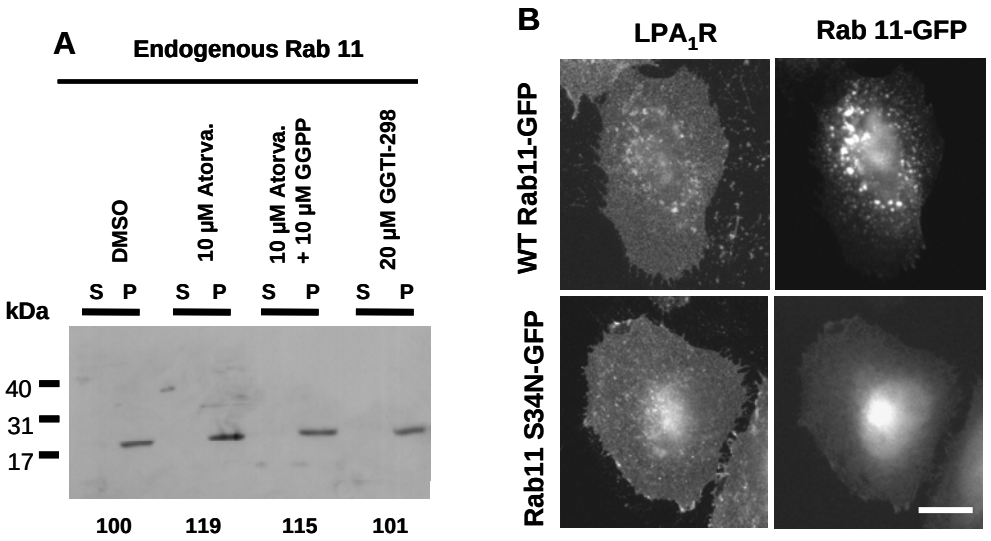

Figure 9: Atorvastatin and GGTI-298 do not reduce the cellular abundance of endogenous Rab 11.

(**A**) Atorvastatin and GGTI-298 do not perturb the partitioning of endogenous Rab11 between soluble and particulate fractions and do not alter the abundance of Rab11. HeLa cells expressing FLAG-LPA_1R were treated with atorvastatin (10µM for 48 h) or GGTI-298 (20 µM for 24 h) and then separated into soluble (S) or particulate (P) fractions prior to western blotting for endogenous Rab11. The numbers below the gels indicate the combined band intensities of the (S+P) fractions for each treatment, which were normalized to the control, vehicle-treated samples. (**B**) Neither overexpression of wild type Rab11-GFP nor dominant inhibitory Rab 11 S34N-GFP induces endosomal sequestration of LPA_1R. Note that whereas wild type Rab 11-GFP associates with large endosomal structures, dominant inhibitory Rab 11 S34N-GFP remains in a diffuse cytoplasmic pattern.

Whereas Rab GTPases are prenylated by Rab geranylgeranyltransferase (Pereira-Leal *et al.*, 2001), which is not inhibited by GGTI-298, Rho GTPases are prenylated by geranylgeranyltransferase-I (Denoyelle *et al.*, 2001; Muck *et al.*, 2004), which is inhibited by GGTI-298. Indeed, most of the anti-cancer effects of statins and GGTIs are due to inhibition of RhoA-related GTPases (e.g., RhoA, B, or C) (Kusama *et al.*, 2001). Given the high sequence identity between RhoA, B, and C (~85%), isoform-specific antibodies are not available. Therefore, we transfected HeLa cells with HA-tagged forms of RhoA, B, or C and examined the effects of atorvastatin and GGTI-298 on the distribution of these tagged GTPases between soluble and particulate fractions (Figure 10). In control cells, both HA-RhoA and HA-RhoC were approximately equally distributed between soluble and particulate fractions, whereas HA-RhoB was predominantly localized to the particulate fraction. Although neither atorvastatin nor GGTI-298 induced a noticeable shift in the distribution of HA-Rho proteins, these inhibitors markedly reduced the total abundance of HA-RhoC (>70% reduction) and HA-RhoA (>60% reduction). These inhibitors also reduced the abundance of HA-RhoB (40-55%), but to a lesser degree than HA-RhoC and HA-RhoA.

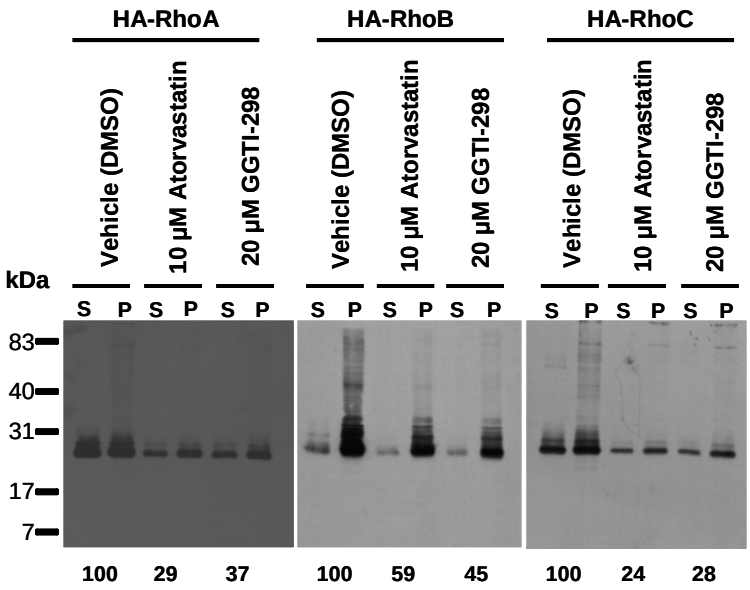

Figure 10: Atorvastatin and GGTI-298 reduce the cellular abundance of HA-RhoA, HA-RhoB, and HA-RhoC.

Atorvastatin and GGTI-298 greatly reduce the cellular abundance of RhoA, B, and C in following rank order: RhoC > RhoA >> RhoB. Cells expressing HA-tagged RhoA, B, or C were treated with atorvastatin (10µM for 48 h) or GGTI-298 (20 µM for 24 h) and then separated into soluble (S) or particulate (P) fractions prior to western blotting. The numbers below the gels indicate the combined band intensities of the (S+P) fractions for each treatment, which were normalized to the control, vehicle-treated samples.

Knockdown of RhoC and RhoA induces the endosomal sequestration of LPA_1Rs but does not affect transferrin receptor trafficking

To determine whether RhoA-related GTPases were involved in the endosomal trafficking of LPA_1Rs, we transiently transfected LPA_1R-expressing HeLa cells with a plasmid that encoded C3 transferase; an exoenzyme derived from *Clostridium botulinum* that selectively ADP-ribosylates and inactivates RhoA, B, and C (Paterson *et al.*, 1990; Aktories and Just, 2005). LPA_1Rs localized to the plasma membrane in cells transfected with a non-specific plasmid, pBluescript, and filamentous actin (F-actin) in these cells was distributed in thin stress fibers and in a band that encircled the cell at the plasma membrane (Figure 11, pBluescript). In cells treated with 10 μM atorvastatin for 48 h, LPA_1Rs were sequestered in endosomes and rhodamine-phalloidin staining of stress fiber was reduced (Figure 11, 10 μM Atorvastatin). In cells expressing C3 transferase, LPA_1Rs were predominantly localized to transferrin-positive endosomes and actin stress fibers were greatly disrupted, indicating that Rho activity was inhibited (Ridley and Hall, 1992). Rhodamine-phalloidin labeled randomly localized punctate spots in the cytoplasm of these cells rather than the thin F-actin filaments observed in control cells. These data support the hypothesis that RhoA-related GTPases regulate the trafficking of LPA_1Rs through recycling endosomes.

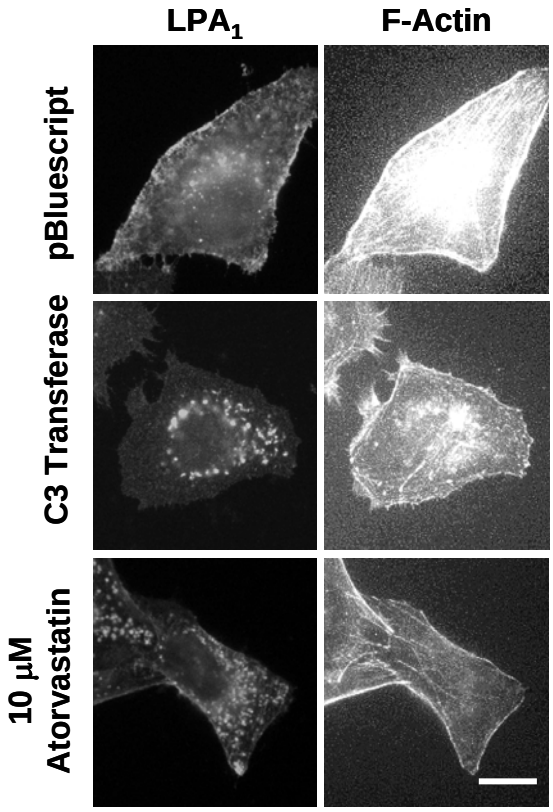

Figure 11: C3 transferase induces the endosomal localization of LPA_1Rs.
Transient transfection of plasmid encoding *Clostridium botulinum* C3 transferase induces the localization of LPA_1Rs to endosomes, similar to 10 μM atorvastatin, and disrupts the actin cytoskeleton as observed by immunofluorescence localization of LPA_1Rs and rhodamine phalloidin staining of F-actin. Bar, 10 μm.

To directly test whether inhibition of RhoA-related GTPases would induce endosomal sequestration of LPA_1R, we used specific siRNAs to knockdown expression of RhoA, B, or C (Figure 12). Since antibodies specific for the individual RhoA-related proteins were not available, we used reverse transcriptase PCR to assess the effects of siRNA treatment on the mRNAs for RhoA, B, and C. In cells transfected with control siRNA, specific DNA fragments for the individual RhoA-related proteins were readily amplified (Figure 12C, control lanes). In contrast, DNA products were not amplified from cells treated with siRNAs specific for the individual RhoA isoforms (Figure 12C, siRNA lanes). Endosomal sequestration was assessed by comparing the localization of LPA_1R to TfnR (Figure 12A). Cells treated with siRNAs specific for RhoA and RhoC showed extensive co-localization of LPA_1R and TfnR, whereas cells treated with siRNA for RhoB showed little co-localization of LPA_1R and TfnR; control siRNA-treated cells showed no co-localization of LPA_1R and TfnR. This suggested that knockdown of either RhoA or RhoC increased the localization of LPA_1R to recycling endosomes.

To quantify this effect, we determined both the number of cells displaying co-localization of LPA_1R and TfnR, in random fields of cells, and the extent of fluorescence pixel overlap between LPA_1R-specific staining and TfnR-specific staining in individual cells (Figure 12B). In cells treated with control siRNAs, the percentage of cells displaying co-localization of LPA_1R and TfnRs were approximately 10% and the average fluorescence pixel overlap in individual cells was about 25%. In contrast, approximately 95% of cells treated with atorvastatin (10 μM) for 48 h displayed co-localization of LPA_1R and TfnR. An average fluorescence pixel overlap of about 80% was observed between LPA_1R and TfnR labeling in individual cells. Remarkably, approximately 80%

of cells treated with siRNA for RhoC showed co-localization of LPA_1R and TfnR, and about 80% pixel overlap between the two proteins was observed in individual cells. Approximately 70% of cells treated with siRNA for RhoA showed co-localization for LPA_1R and TfnR and a little more than 60% fluorescence pixel overlap. Cells treated with siRNA for RhoB displayed co-localization of LPA_1R and TfnR in about 35% of cells and about 50% fluorescence pixel overlap. These results indicate that siRhoC was the most potent inducer of endosomal sequestration of LPA_1R, whereas siRhoA was slightly less potent than siRhoC at inducing endosomal sequestration. SiRhoB was not nearly as potent as either siRhoC or siRhoA in inducing endosomal sequestration of LPA_1R. Given that RhoB has been implicated in trafficking from early endosomes to lysosomes (Mellor *et al.*, 1998; Gampel *et al.*, 1999; Fernandez-Borja *et al.*, 2005), it is probable that perturbing RhoB function has indirect effects on trafficking through recycling endosomes. Finally, we tested the effects of siRhoA, siRhoB, and siRhoC on the endocytosis and recycling of Alexa594-Tfn (Figure 13). In contrast to the sequestration of LPA_1Rs observed in siRhoA- and siRhoC-treated cells, neither Alexa-Tfn internalization (Load) nor recycling (Chase) was altered by siRNA-mediated reduction of these two GTPases. Taken together, these results suggest that RhoA and RhoC are critical for LPA_1R trafficking through recycling endosomes but not for transferrin receptor trafficking.

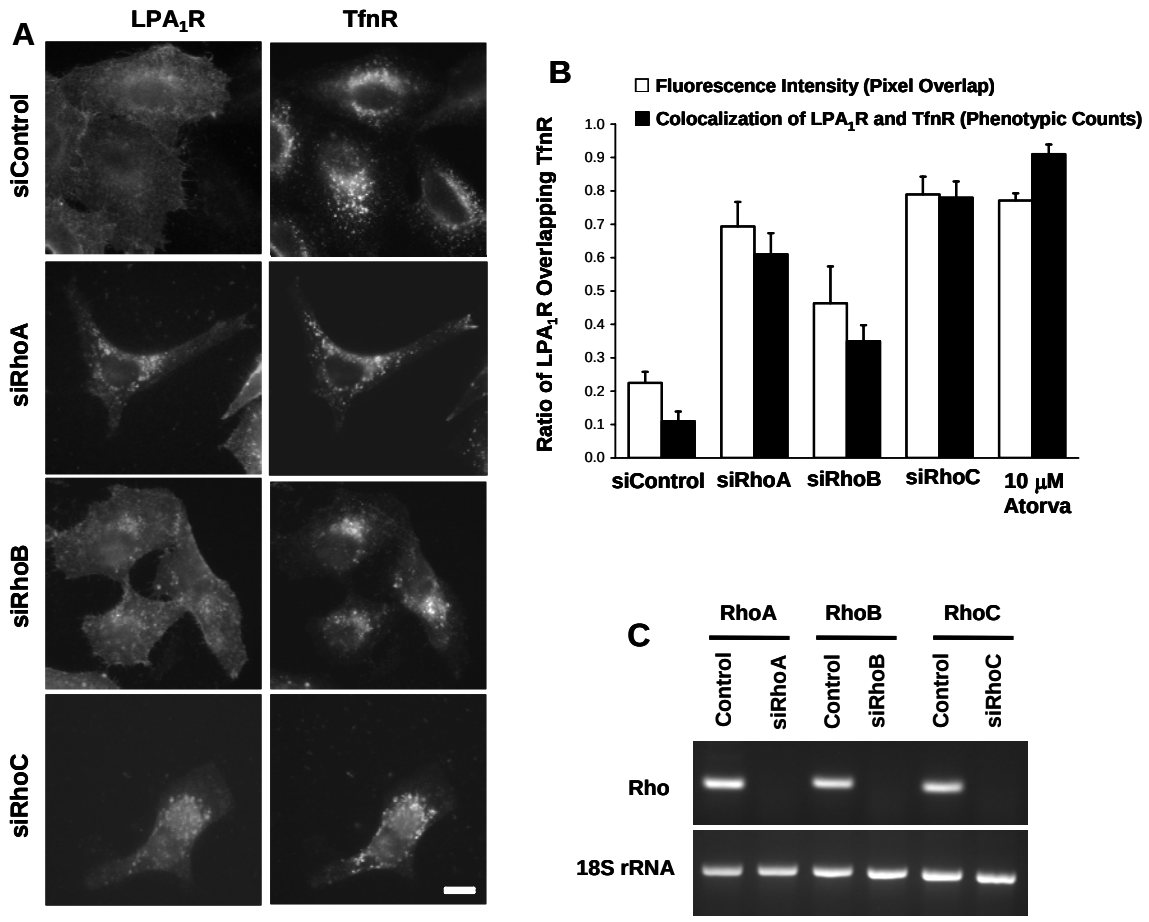

Figure 12: Depletion of cellular RhoA or RhoC induces endosomal sequestration of LPA_1R.

(**A**) SiRNA knockdown of RhoA or RhoC induces the endosomal co-localization of LPA_1R and TfnRs. Knockdown of RhoB partially induces the localization of LPA_1R to Tfn^+ recycling endosomes. (**B**) SiRNA reduction of RhoA, B, and C increases the sequestration of LPA_1R in $TfnR^+$ recycling endosomes. Endosomal sequestration was quantified by phenotypic counting (100 cells/condition) and by measurement of fluorescence pixel overlap (9 cells/condition). The values are the means ± s.e.m. from a representative experiment that was repeated three times with similar results. (**C**) RT-PCR analysis shows that specific siRNA treatment eliminates the expression of RhoA, RhoB, and RhoC mRNA.

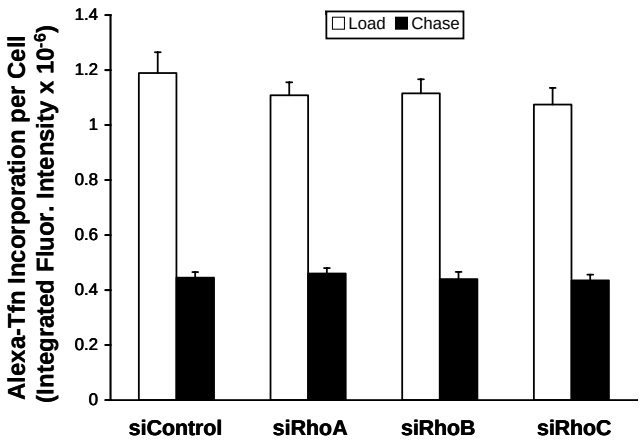

Figure 13: Depletion of RhoA, RhoB, or RhoC does not affect transferrin recycling. SiRNA reduction of RhoA, B, or C did not affect the internalization or recycling of Alexa-Tfn. Cells were incubated with Alexa-Tfn (20 μg/ml, 30 min, "Load", white bars), rinsed and either fixed or incubated in medium containing excess unlabeled transferrin and the iron chelator, desferroxamine, for 2 hr (Chase, black bars) prior to fixation. The fluorescence intensity of cell-associated Alexa-Tfn was quantified from 15 cells per condition from a representative experiment.

CHAPTER 4

DISCUSSION

We have shown that atorvastatin, mevastatin, GGTI-298, and siRNA knockdown of RhoC and RhoA lead to a novel endosomal sequestration of cell surface LPA_1R receptors. The most likely cause for the sequestration of LPA_1Rs, as well as β_2ARs and M_2 mAChRs, in endosomes, is through inhibition of receptor recycling, which leads to the trapping of receptors that are internalized during basal endocytosis, in recycling endosomes. Atorvastatin, mevastatin, and GGTI-298 lead to defects in protein geranylgeranylation, either by depletion of geranylgeranylpyrophosphate, which is required for protein geranylgeranylation, or by direct inhibition of geranylgeranyltransferase-I, respectively. RhoA and RhoC are both prenylated by geranylgeranyltransferase-I (Braun *et al.*, 1989; Chardin *et al.*, 1989; Aktories *et al.*, 2004). Taken together, we hypothesize that atorvastatin and GGTI-298 induce endosomal sequestration by preventing the geranylgeranylation of RhoC and RhoA, which inhibits their function and leads to the inhibition of receptor recycling.

Statins are the most widely prescribed class of prescription drugs in the world and have traditionally been used to lower blood cholesterol in patients. The peak plasma concentration of atorvastatin prescribed for cholesterol reduction in patients ranges from 0.02 to 0.05 μM (Corsini *et al.*, 1999). The lowest concentration of atorvastatin, which induces endosomal sequestration of LPA_1Rs, is 0.1 μM (unpublished observations; P.D.S and H.R.). This is at least a 5-fold higher concentration of atorvastatin than is used for therapeutic reduction of cholesterol in patients. The major side effects of high dose statin

treatment are myopathy and rhabdomyolysis, typically in striated muscle (Kusama *et al.*, 2001). Given that 10- to 100-fold higher concentrations of atorvastatin were required to observe GPCR sequestration, *in vitro*, we do not expect that plasma concentrations of atorvastatin in patients approach levels where this type of receptor sequestration occurs *in vivo*, with the caveat that localized increases in atorvastatin concentration may occur in certain areas of the body. Rather, our data indicate that atorvastatin at these higher concentrations is a very useful experimental tool to investigate endosomal recycling *in vitro*.

Inhibition of HMG-CoA reductase depletes the downstream products of the mevalonate pathway, which include not only sterols but also retinoids, ubiquinone, dolichols, and the isoprenoids, farnesylpyrophosphate and geranylgeranylpyrophosphate (Chan *et al.*, 2003). The latter products are utilized for protein prenylation. Recently, statins have gained wide interest as anti-cancer agents and have been shown to inhibit the growth and migration of a broad range of cancer cells *in vitro*, including those from breast cancer (Denoyelle *et al.*, 2001), lymphoma (Matar *et al.*, 1999), and glioblastoma (Kikuchi *et al.*, 1997).

Many Rho GTPases have been implicated in the regulation of membrane trafficking (Symons and Rusk, 2003). RhoA, Rac, and Cdc42 have been implicated in endocytosis from the plasma membrane, whereas RhoB and RhoD are involved in endosomal trafficking. RhoD regulates the distribution and motility of early endosomes (Murphy *et al.*, 1996; Murphy *et al.*, 2001). Constitutively active mutants of RhoA and Rac1 are potent inhibitors of transferrin receptor endocytosis (Lamaze *et al.*, 1996). The downstream Rac effector, synaptojanin2, is involved in Rac1 regulation of transferrin

receptor endocytosis (Malecz *et al.*, 2000). RhoB has been shown to regulate the trafficking of EGF receptors from early endosomes to lysosomes through effects on F-actin assembly (Gampel *et al.*, 1999; Fernandez-Borja *et al.*, 2005). The Cdc42 effector, ACK1 kinase, also interacts with clathrin heavy chain and can influence transferrin receptor endocytosis (Teo *et al.*, 2001).

In this study, we observed that siRNA-mediated reduction of RhoC or, to a lesser degree, RhoA led to sequestration of LPA_1R in recycling endosomes (Figure 12). These observations were further strengthened by the finding that transient transfection of C3 transferase, which inhibits RhoA-related proteins, also induced a sequestration of LPA_1Rs in recycling endosomes (Figure 11). In contrast, neither dominant inhibitory mutants of Rac1 (T17N) nor Cdc42 (T17N) induced endosomal sequestration of LPA_1R (P.D.S. and H.R., unpublished observations). The finding that reduction of either RhoA or RhoC induced endosomal sequestration of LPA_1R suggests a functional overlap between these proteins (Figure 12). It is interesting to note that RhoA and RhoC cooperate to promote proliferation and invasiveness, respectively, of esophageal squamous cell carcinoma cells and certain breast cancer cell lines (Pille *et al.*, 2005; Faried *et al.*, 2006). The identification of RhoC as an important regulator of endosomal trafficking raises the novel possibility that this RhoC function is also important for the stimulation of cancer cell invasion. RhoC is overexpressed in a variety of metastatic and invasive cancers including: breast (Pille *et al.*, 2005), ovarian (Horiuchi *et al.*, 2003), and pancreatic ductal cancers (Suwa *et al.*, 1998), as well as melanoma (Collisson *et al.*, 2003; Ruth *et al.*, 2006); however, its precise role in stimulating cancer cell invasion is not clear.

The mechanisms by which RhoC and RhoA regulate GPCR trafficking through recycling endosomes are not clear. Another RhoA-related GTPase, RhoB, has been shown to regulate the trafficking of EGF receptors from early endosomes to lysosomes by mediating the assembly of F-actin around endosomes, via the formin protein, mDia1 (Fernandez-Borja *et al.*, 2005), and through the action of the protein kinase, PRK1 (Mellor *et al.*, 1998). The exact role of PRK1 in endosomal trafficking is unknown. RhoB- and Dia1-mediated actin assembly on endosomal structures is thought to link endosomes to F-actin fibers and perhaps coordinate endosome motility (Fernandez-Borja *et al.*, 2005). RhoA, B, and C share about 85% amino acid identity and interact with most of the same effector proteins. Thus, it is possible that RhoC and RhoA utilize a similar mechanism and/or effectors in the regulation of recycling endosomal trafficking as RhoB.

An important distinction to note is that while atorvastatin and knockdown of RhoA and RhoC perturbed the trafficking of GPCRs (e.g., induced endosomal sequestration), these treatments did not perturb the internalization or recycling of Alexa-transferrin (Figures 8 and 13). This suggests that GPCR trafficking through recycling endosomes is perhaps regulated differently from transferrin receptors. Indeed, dominant inhibitory Rab11 S34N can inhibit the recycling of transferrin receptors (Ullrich *et al.*, 1996), but does not induce endosomal sequestration of LPA_1R receptors (Figure 9B). Mechanistic details about trafficking through recycling endosomes are beginning to emerge. In addition to the Rab11 GTPase, RME-1 and its human homologue, EHD1, localize to recycling endosomes and are important regulators of endocytic recycling (Lin *et al.*, 2001). The RME-1 protein was identified in a genetic screen in *C. elegans* for

endocytosis mutants, and dominant negative RME-1/EHD1 slowed TfnR recycling and altered the cellular distribution of recycling endosomes (Grant *et al.*, 2001). Rabenosyn-5, a Rab4/Rab5 effector, physically interacts with EHD1 and is thought to act sequentially with EHD1 in mediating trafficking from early endosomes to recycling endosomes and subsequently to the plasma membrane (Naslavsky *et al.*, 2004a).

In conclusion, we have described a process whereby inhibition of protein geranylgeranylation, with atorvastatin or GGTI-298, leads to a novel sequestration of multiple GPCRs in recycling endosomes. We speculate that the defective prenylation of the RhoA-related GTPases, RhoC and RhoA, is the cause of statin- and GGTI-mediated endosomal sequestration since siRNA knockdown of either of these two GTPases also causes GPCR sequestration in recycling endosomes. Interestingly, none of these perturbations altered transferrin receptor internalization and recycling, which suggests that different mechanisms of regulation are involved in the trafficking of GPCRs and transferrin receptors from recycling endosomes. Future studies are expected to reveal not only the role of RhoC and RhoA in endocytic recycling but also the relationship between Rab11-regulated and Rho-regulated recycling.

CHAPTER 5

FUTURE DIRECTIONS

We have shown that RhoA, B, and C play a role in the endocytic trafficking of LPA_1Rs. In the results described above, we have not monitored the prenylation state of RhoA, B, and C in response to statin and GGTI treatment. Thus, a potential future study would be to quantitatively determine the levels of endogenous RhoA, B, and C present, and their level of prenylation, in control, statin, and GGTI treated cells. It is important to note that prenylation of RhoB is achieved by attaching a geranylgeranyl group that is 20 carbons in length or a farnesyl group that is 15 carbons in length. In contrast, prenylation of RhoC and A is achieved by attachment of a geranylgeranyl group (Adamson *et al.*, 1992). To test this, we would measure the level of geranylgeranylation of RhoA, B, and C, and also measure the level of farnesylation of RhoB. The expected result of GGTI treatment would be a decrease in the pool of geranylgeranylated-RhoB, and an increase in the pool of farnesylated-RhoB. These studies will more closely link the trafficking effects that we have observed, in response to statin and GGTI treatment, with direct impacts on RhoA, B, and C.

Since we have identified RhoC and A as participants in the regulation of endocytic recycling, the next step will be to identify the specific effector proteins that regulate endocytic trafficking. Immunofluorescence labeling could be utilized in initial experiments to examine the localization of possible effectors in both control cells and cells that have been treated with statin or GGTI. If we observe effectors that localize to endosomes in control cells, but lose the endosomal localization with statin or GGTI treatment, it would indicate that these effectors are possibly recruited to endosomes by

active, prenylated RhoC or A. One method to determine which effectors may be modulating trafficking would be to overexpress inactive mutant forms of potential effectors and examine their effects on trafficking. Further studies could utilize siRNA directed against specific effectors to help determine their functions in endocytic trafficking of LPA_1 receptors. The results of these studies will help us form a better model of the mechanisms that drive endocytic trafficking of LPA_1 receptors.

One interesting possibility is that RhoC and A are functionally equivalent. There is evidence that the gene encoding RhoC resulted from an incomplete duplication of the gene encoding RhoA (Karnoub *et al.*, 2004). However, it is also possible that both RhoC and A are required for recycling of LPA_1Rs to the cell surface, possibly by recruiting slightly different pools of effectors. Our results have shown that siRNA knockdown of either RhoC or A results in the sequestration of LPA_1Rs. If RhoC and A were perfectly functionally interchangeable, it would be reasonable to expect that one would compensate for the other and we would not see sequestration resulting from knockdown of either protein individually. A possible explanation is that RhoC and A function at two different, but closely related steps. One possible mechanism is that one of the two Rho proteins (RhoC or A) could be involved with sorting the receptors into developing vesicles, while the other Rho protein (RhoC or A) may be involved with the recruitment of coat proteins that will pinch the vesicle off from the compartment. Another possibility is that a Rho protein mediates the interaction of transport vesicles with a motor protein that carries the vesicles along the cytoskeleton. One potential study to examine these possibilities would be to visualize the localization of LPA_1Rs in fine detail using immunogold electron microscopy (EM), in response to siRhoA, siRhoB, and siRhoC, both individually and in

combination. The results of this study would help to place RhoA, B, and C at potentially distinct points in the trafficking pathway of LPA_1Rs.

Overall, we have identified a novel role for RhoC and A in the endocytic recycling of GPCRs. This is the first demonstration, of which we are aware, of a role for Rho proteins in endocytic recycling and will hopefully lead to future developments in the understanding of the dynamic processes by which receptors are returned to the cell surface.

APPENDIX A

PROTOCOLS

Splitting mammalian cells

1. Aspirate media and add 2 mL trypsin and incubate for 2-3 minutes at 37 °C.
2. Add 4 mL complete media to cells and pipet cells 20 times to get uniform suspension.
3. Add 0.4-1.0 mL suspended cells to 10 cm dish containing 10 mL of complete media.
4. Label dish with date, split number, cell line, dilution, and initials.
5. If using cells for experimental purposes, count number of cells using hemacytometer.

Plating mammalian cells

1. Flame ethanol soaked coverslips and let air dry for a few seconds before adding to 10 cm dish or 6-well plate.
2. After counting number of cells, place appropriate amount of cells into a conical tube containing media and mix well.
3. Dispense 2 mL or 6 mL of cells into 6-well plate or 10 cm dish, respectively.

Freezing back stocks of mammalian cells

1. Wipe the work area, bottle tops, and gloves very well with ethanol.
2. Aspirate media from cell dish or flask.
3. Rinse cells with enough trypsin to just cover the bottom of the flask.
4. Aspirate off trypsin to remove residual media.
5. Cover flask trypsin and incubate in CO_2 chamber for 2-3 minutes.
6. Add complete media to flask (approx. 2 times the amount of trypsin used) to neutralize trypsin.
7. Label cryogenic tubes with cell line name, date, and your initials.
8. Place cells into chilled 50 mL Corning tube.
9. Centrifuge cells at 1200rpm, 4 °C for 5 min.
10. Aspirate off media with sterile pastuer pipet.
11. Resuspend pellet in 5 ml freezing media (10% DMSO, 90% Fetal Bovine).
12. Aliquot 1 ml of cells into cryogenic tubes VERY CAREFULLY!!!
13. Place in Styrofoam container and place into -80 °C for 3 days.
14. Move tubes to liquid nitrogen for storage.

ExGen 500 transfection

Considerations:

1. 1. High quality DNA of 1.8 OD ratio or higher is recommended.
2. 2. Recommended cell density is around 50% at time of transfection.
3. 3. Optimal detection of transfection can be determined by a reporter gene.
4. 4. Transfection efficiency is higher in the presence of serum without antibiotics.

Day 1: Seed 0.45x 10^6 HeLa cells (density depends on cell type) in a 10 cm dish containing complete DMEM (-antibiotics).
Day 2: Transfect in the morning. Prior to transfection, transfer coverslips to a 6-well plate containing 2 mL of complete DMEM (-antibiotics).
Day 3: Change the media.
Day 4: Perform the assay.
Day 2: Procedure for 6-well plate: Use 1 μg to 3.3 μl ratio of DNA to Ex-Gen.

1. Dilute recommended amount of DNA (Total 2.0 μg/6-well) into 200 μl of 150 mM NaCl.
2. Vortex briefly and spin down.
3. Add 7.0 μl of ExGen500 to DNA solution and immediately vortex for 10 sec.
4. Incubate at room temperature for 10 min.
5. Add the ExGen500/DNA mixture to one well of 6-well plate and place on shaker for 5 min.
6. Incubate for 24 h and change media following day.
7. Assay 48 h after transfection.

Internalization of Alexa-labeled human transferrin

1. Plate cells on 12 nm circle (No. 1) coverslips and grow until experiment in complete culture medium (containing FBS, antibiotics, etc.).
2. Transfer individual coverslips to wells in 12 well dish.
3. Rinse cells 3x with serum-free medium containing 0.5% BSA (BSA/SFM).
4. Incubate cells in BSA/SFM for 30 min at 37 °C. (This step chases out the native transferring bound to the endogenous receptors.) Add any drug treatments at this time as well.
5. Add 10μl of a 50mg stock of Alexa-Labeled Transferrin (in molecular probes box stored at 4°C).
6. Incubate cells at 37 °C for 20min.
7. Rinse cells briefly with 0.5% acetic acid, 0.5 M NaCl, and then several times with complete medium (containing serum).
8. Fix for 10 min with 2% formaldehyde in PBS.
9. Rinse for 5 min with 1X PBS.
10. Mount coverslips on slide.

Indirect immunofluorescence

1. Day 1: Plate 0.10 x 10^6 HeLa, 0.13 x 10^6 MEF wt, 0.08 x 10^6 MEF KO 1/2 cells on flamed 12 mm circle glass coverslips in a 6-well dish.
2. Day 2: Begin transfection protocol according to manufacturer's protocol.
3. Day 3: Treat as required for experimental protocol.
4. Transfer coverslips to a 12-well dish containing 1 mL of chilled 2% formaldehyde in PBS pH 7.4
5. Incubate for 10 minutes at room temperature.
6. Remove fixative and add 1 mL of 10% adult calf serm and 0.02% sodium azide in PBS (PBS/serum).
7. Incubate for 5 minutes at room temperature.
8. Dilute primary antibodies into PBS/serum containing 0.2% saponin and spin for 5 minutes at 14,000 rpm.
9. Add parafilm to the bottom of a 150 mm Petri dish and label for each corresponding coverslip in the 12-well plate.
10. Add 25 µl of the diluted antibody solution to appropriate spot on the parafilm.
11. Using forceps pick up individual coverslips, wick off excess fluid on paper towel, and add cell side down directly onto 25 µl of diluted antibody.
12. Place cover on 150 mm Petri dish and incubate for 45 minutes.
13. Carefully transfer coverslip, cell-side up, back into 12-well dish containing PBS/serum.
14. Wash cells with 1 mL PBS/serum (3 x for 5 minutes)
15. Dilute fluorescently-labeled secondary antibodies in PBS/serum + 0.2% saponin and spin for 5 minutes at 14,000 rpm.
16. Invert coverslips onto 25 µl of diluted secondary on parafilm as described above.
17. Incubate for 45 minutes.
18. Wash coverslips 3 x 5 minutes with PBS/serum.
19. Rinse coverslips with 1X PBS and mount onto glass slides with fluoromount G.
20. Seal edges of coverslips with clear nail polish.

Metamorph colocalization

1. Open and load image of interest
   Deconvolute images prior to quantitation
2. Process Menu
   Select "2D deconvolution"
   Click nearest neighbor and Apply (adjust if needed)
   Display color combine
3. Display Menu
   Select "Color Separate"
   Click red, green or blue ---"new"
4. Select rectangle box in Regions tools and place in Blank region of image
5. Regions Menu
   Select "Transfer Region" to place blank in all colors of image

6. Measure Menu
   Select "Show Region Statistics"
   *the "Use Threshold" box should NOT be checked
   *region around box should be blinking (active)
   *Add the sum of average and standard deviation computed for each color image.
   Record measurements for each color.
7. Measure Menu
   Select "Threshold Image"
   *Make sure State is Off
   Insert the values derived from previous step into the "Low Intensity" box
8. Region Tools
   Select line or box tool to mark the areas of image to analyze. Double click to activate.
9. Regions Menu
   With image outline blinking, select Transfer Region
   Transfer outline of interest to all the color images separated earlier
10. Measure Menu
    Select "Show Region Statistics"
    *Check the "inclusive" box for each color of the image
    * Add the sum of the average and standard deviation computed
11. Measure Menu
    Select "Threshold Image"
    *input the sum calculated above into the "Low intensity" box
12. Applications Menu
    Select "Measure colocalization"
    *set image to "A" or "B" as appropriate
    *check the "show percentage box"
    *log into Excel spreadsheet

Fractionation of total membranes and cytosol

1. Rinse cells twice with ice-cold PBS on ice/H_2O bath.
2. Add 4 ml cold PBS and scrape cells, add to a cold 15 ml screw-cap tube. Rinse cells with 2 ml PBS and add to tube.
3. Pellet cells (1200 rpm, 5 min in Sorvall RT6000D table top = 300 x g).
4. Resuspend cells in 2 ml of (250 mM sucrose, 10mM Tris-Cl pH 7.4).
5. Pellet cells as described in step 3.
6. Resuspend cells in ~ 500 µl of (100 mM sucrose, 10 mM Tris-Cl pH 7.4). [You should vary the volume you resuspend the cells in depending on how many cells you have (e.g., resuspend in less (~ 200 µl) if you have fewer cells).]
7. Transfer suspension to a small petri dish on ice.
8. Break cells by passing suspension through 25 guage syringe needle attached to a 1 ml syringe (up/down 5-10 times for HeLa cells, 10-15 for Cos or NRK cells). Examine under scope to check for breakage.
9. Transfer to chilled microfuge tube, centrifuge in Biofuge at 4°C (speed 3.5, 5 min).

10. Transfer the postnuclear supernatant (PNS) to chilled microfuge tube. At this point, you can split PNS into aliquots (120 µl) for various treatments or manipulations. Remember to always save some of PNS for gel.
11. Transfer 120 µl aliquots of PNS to ultracentrifuge tubes (Beckman Polyallomer tubes).
12. Centrifuge in a TLA 100.2 rotor in table top ultracentrifuge at 60,000 rpm ~ 150,000 x g (30 min, 4°C.)
13. Remove supe (cytosol, 120 µl) and add 40 µl of 4x SDS sample buffer.
14. Solubilize pellet (total membranes) in 160 µl 1x SDS sample buffer.
15. Boil samples 3 min at 95 °C.
16. Separate by electrophoresis (use 13% gels for small GTPases).

Solutions	20 ml
250 mM sucrose 10 mM Tris-Cl pH 7.4 final	5 ml of 1 M stock 0.2 ml of 1 M stock → add dH_2O to 20 ml
100 mM sucrose 10 mM Tris-Cl pH 7.4 final	2 ml of 1 M stock 0.2 ml of 1 M stock → add dH_2O to 20 ml

Cell lysis for Western blotting

1. Rinse culture dishes of cells twice with ice-cold 1X PBS
2. Scrape cells into a pool at the bottom of the dish using 1X PBS with protease and phosphatase inhibitors added fresh each time
3. Transfer pool of cells into an ice-cold microfuge tube and spin in a cold centrifuge at 500-1200 rpm for about 5-15 min.
4. Add 200-500 µl (HeLa) of lysis buffer to the cell pellet after removing the supernatant.

   Lysis Buffer:
   1% NP-40 1mL
   1% deoxycholate salt 1g
   0.15M NaCl (from 5M stock) 3mL
   0.1% SDS (from 20% stock) 0.5mL
   0.01M sodium phosphate 7.2 10mL
   2mM EDTA (from 0.5M stock) 400µl
   50mM NaF (from 1M stock) 5mL
   0.2M orthovanadate (from 0.1M stock) 2mL
   H_2O (to 100mL total volume) 78mL
   *Add fresh protease inhibitors each time
5. Allow the cells to lyse on ice for 30 min with vortexing every 10 min.
6. Spin in the cold centrifuge for 15 min, remove supernatant for BCA Assay.

SDS-PAGE gel recipe

MINIGEL: SEPARATING GEL (10 mL)

Reagent:	7%	10%
40% Acrylamide	1.75 mL	2.5 mL
1.5M Tris, 0.4% SDS pH 8.8	2.5 mL	2.5 mL
ddH_2O	5.25 mL	5.0 mL
10% APS *fresh	50 µl	50 µl
TEMED	10 µl	10 µl

MINIGEL: STACKING GEL (5 mL)

Reagent:	
40% Acrylamide	0.375 mL
0.5M Tris, 0.4% SDS pH 6.8	1.25 mL
ddH_2O	3.375 mL
10% APS *fresh	50 µl
TEMED	7.5 µl

SDS-PAGE setup

1. Assemble two glass plates using green casting stand from Bio-Rad.
2. Place cast upright in the Bio-Rad assembly stand to seal bottom of gel.
3. Pour mixed separating gel using a Pasteur pipet ensuring no air bubbles form.
4. Overlay gel with isopropanol to ensure a flat surface and to exclude air.
5. Allow ~45 minutes for gel to polymerize.
6. Pour stacking gel onto top of set separating gel and insert comb.
7. Allow gel to set. May store gel overnight at 4^0C.
8. Place one or two gels into the slots of the Mini Tran Blot Cell, ensuring that the short plate faces the interior of the cell.
9. Remove comb and remove bubbles from wells using a syringe.
10. Load 5 µl of protein standard and ~20 µl of protein sample to corresponding wells.
11. Fill the middle buffer chamber with 1X SDS running buffer (196 mM glycine, 50 mM Tris-Cl pH 8.3, 0.1% SDS). Once running buffer reaches lanes slowly add rest of running buffer and ensure that samples do not run over into adjacent lanes. Fill to top.
12. Fill the lower buffer chamber with 1X SDS running buffer until it covers the wire found on the inside of the gel apparatus.
13. Connect the electrode cables to power supply.
14. Run gel at 150V for ~1 hour or until dye runs off gel.

Western Blotting with chemiluminescence detection

1. Following SDS-PAGE, carefully separate glass plates and float the gel off the glass plate under chilled transfer buffer.
2. Assemble sandwich in this order on top of black side of sandwich.

a. Scotch-brite pad (presoaked in transfer buffer)
b. Whatman filter paper (presoaked in transfer buffer)
c. SDS-PAGE Gel
d. Nitrocellulose paper (presoaked in transfer buffer)
    i. Roll out air bubbles
e. Whatman filter paper (presoaked in transfer buffer)
f. Scotch-brite pad

3. Seal cassette, place in Mini Protean II Cell, fill with chilled transfer buffer, and add ice pack.
4. Connect the electrode cables to power supply.
5. Run gel at 50V for 1.5 hours or until loading dye just runs off of bottom of gel.
6. Transfer nitrocellulose to blocking buffer (Tris buffered saline with 0.1% Tween 20 (0.1% TBST) and 2% milk)
7. Block nitrocellulose for 2 hours at room temperature on rocking platform.
8. Transfer nitrocellulose to ziplock bag containing diluted primary antibody in 10 mL of blocking buffer.
9. Incubate on rocker overnight at 4 °C.
10. Wash nitrocellulose 2Xs with 0.1% TBST.
11. Incubate with secondary antibody diluted in blocking buffer for 1 hour on rocker at room temperature. (HRP conjugated donkey 1:5000)
12. Wash nitrocellulose 3Xs with 0.1% TBST.
13. Treat on plastic wrap with West Pico solution (1:1 mixture of Solution A and Solution B; made up just before use) for 5 minutes.
14. Transfer nitrocellulose to plastic wrap and place in film cassette and go to dark room.
15. Expose film for 1 minute and increase or decrease exposure time as needed.
16. Develop film using the automated developer in the dark room.

BCA assay

1. Add 0, 5, 10, 15, 20 µl of 1 mg/mL of BSA standard to corresponding wells in a 96-well plate.
2. Add 5 µl of protein sample (lysate) to 96-well plate.
3. Add 200 µl of BCA mixture to each well containing sample. (1 part solution B to 50 parts solution A.)
4. Incubate plate for 30 minutes at 37 °C.
5. Read plate at 562 nm using a microplate reader.

REFERENCES

Adamson, P., Marshall, C.J., Hall, A., and Tilbrook, P.A. (1992). Post-translational modifications of p21rho proteins. J Biol Chem *267*, 20033-20038.

Ahn, S., Nelson, C.D., Garrison, T.R., Miller, W.E., and Lefkowitz, R.J. (2003). Desensitization, internalization, and signaling functions of beta-arrestins demonstrated by RNA interference. Proc Natl Acad Sci U S A *100*, 1740-1744.

Aktories, K., and Just, I. (2005). Clostridial Rho-inhibiting protein toxins. Curr Top Microbiol Immunol *291*, 113-145.

Aktories, K., Wilde, C., and Vogelsgesang, M. (2004). Rho-modifying C3-like ADP-ribosyltransferases. Rev Physiol Biochem Pharmacol *152*, 1-22.

Benovic, J.L., Kuhn, H., Weyand, I., Codina, J., Caron, M.G., and Lefkowitz, R.J. (1987). Functional desensitization of the isolated beta-adrenergic receptor by the beta-adrenergic receptor kinase: potential role of an analog of the retinal protein arrestin (48-kDa protein). Proc Natl Acad Sci U S A *84*, 8879-8882.

Bishop, A.L., and Hall, A. (2000). Rho GTPases and their effector proteins. Biochem J *348 Pt 2*, 241-255.

Bonifacino, J.S., and Traub, L.M. (2003). Signals for sorting of transmembrane proteins to endosomes and lysosomes. Annu Rev Biochem *72*, 395-447.

Braun, U., Habermann, B., Just, I., Aktories, K., and Vandekerckhove, J. (1989). Purification of the 22 kDa protein substrate of botulinum ADP-ribosyltransferase C3 from porcine brain cytosol and its characterization as a GTP-binding protein highly homologous to the rho gene product. FEBS Lett *243*, 70-76.

Cannizzaro, L.A., Madaule, P., Hecht, F., Axel, R., Croce, C.M., and Huebner, K. (1990). Chromosome localization of human ARH genes, a ras-related gene family. Genomics *6*, 197-203.

Cao, T.T., Deacon, H.W., Reczek, D., Bretscher, A., and von Zastrow, M. (1999). A kinase-regulated PDZ-domain interaction controls endocytic sorting of the beta2-adrenergic receptor. Nature *401*, 286-290.

Casey, P.J., and Seabra, M.C. (1996). Protein prenyltransferases. J Biol Chem *271*, 5289-5292.

Chan, K.K., Oza, A.M., and Siu, L.L. (2003). The statins as anticancer agents. Clin Cancer Res *9*, 10-19.

Chardin, P., Boquet, P., Madaule, P., Popoff, M.R., Rubin, E.J., and Gill, D.M. (1989). The mammalian G protein rhoC is ADP-ribosylated by Clostridium botulinum exoenzyme C3 and affects actin microfilaments in Vero cells. Embo J *8*, 1087-1092.

Collisson, E.A., Kleer, C., Wu, M., De, A., Gambhir, S.S., Merajver, S.D., and Kolodney, M.S. (2003). Atorvastatin prevents RhoC isoprenylation, invasion, and metastasis in human melanoma cells. Mol Cancer Ther *2*, 941-948.

Corsini, A., Bellosta, S., Baetta, R., Fumagalli, R., Paoletti, R., and Bernini, F. (1999). New insights into the pharmacodynamic and pharmacokinetic properties of statins. Pharmacol Ther *84*, 413-428.

Denoyelle, C., Vasse, M., Korner, M., Mishal, Z., Ganne, F., Vannier, J.P., Soria, J., and Soria, C. (2001). Cerivastatin, an inhibitor of HMG-CoA reductase, inhibits the signaling pathways involved in the invasiveness and metastatic properties of highly invasive breast cancer cell lines: an in vitro study. Carcinogenesis *22*, 1139-1148.

Fang, X., Gaudette, D., Furui, T., Mao, M., Estrella, V., Eder, A., Pustilnik, T., Sasagawa, T., Lapushin, R., Yu, S., Jaffe, R.B., Wiener, J.R., Erickson, J.R., and Mills, G.B. (2000). Lysophospholipid growth factors in the initiation, progression, metastases, and management of ovarian cancer. Ann N Y Acad Sci *905*, 188-208.

Faried, A., Faried, L.S., Kimura, H., Nakajima, M., Sohda, M., Miyazaki, T., Kato, H., Usman, N., and Kuwano, H. (2006). RhoA and RhoC proteins promote both cell proliferation and cell invasion of human oesophageal squamous cell carcinoma cell lines in vitro and in vivo. Eur J Cancer *42*, 1455-1465.

Ferguson, S.S. (2001). Evolving concepts in G protein-coupled receptor endocytosis: the role in receptor desensitization and signaling. Pharmacol Rev *53*, 1-24.

Fernandez-Borja, M., Janssen, L., Verwoerd, D., Hordijk, P., and Neefjes, J. (2005). RhoB regulates endosome transport by promoting actin assembly on endosomal membranes through Dia1. J Cell Sci *118*, 2661-2670.

Furberg, C.D., and Pitt, B. (2001). Withdrawal of cerivastatin from the world market. Curr Control Trials Cardiovasc Med *2*, 205-207.

Gage, R.M., Matveeva, E.A., Whiteheart, S.W., and von Zastrow, M. (2005). Type I PDZ ligands are sufficient to promote rapid recycling of G Protein-coupled receptors independent of binding to N-ethylmaleimide-sensitive factor. J Biol Chem *280*, 3305-3313.

Gampel, A., Parker, P.J., and Mellor, H. (1999). Regulation of epidermal growth factor receptor traffic by the small GTPase rhoB. Curr Biol *9*, 955-958.

Ghosh, R.N., Mallet, W.G., Soe, T.T., McGraw, T.E., and Maxfield, F.R. (1998). An endocytosed TGN38 chimeric protein is delivered to the TGN after trafficking through the endocytic recycling compartment in CHO cells. J Cell Biol *142*, 923-936.

Goetzl, E.J., Lee, H., Dolezalova, H., Kalli, K.R., Conover, C.A., Hu, Y.L., Azuma, T., Stossel, T.P., Karliner, J.S., and Jaffe, R.B. (2000). Mechanisms of lysolipid phosphate effects on cellular survival and proliferation. Ann N Y Acad Sci *905*, 177-187.

Grant, B., Zhang, Y., Paupard, M.C., Lin, S.X., Hall, D.H., and Hirsh, D. (2001). Evidence that RME-1, a conserved C. elegans EH-domain protein, functions in endocytic recycling. Nat Cell Biol *3*, 573-579.

Hajdo-Milasinovic, A., Ellenbroek, S.I., van Es, S., van der Vaart, B., and Collard, J.G. (2007). Rac1 and Rac3 have opposing functions in cell adhesion and differentiation of neuronal cells. J Cell Sci *120*, 555-566.

Hama, K., Aoki, J., Fukaya, M., Kishi, Y., Sakai, T., Suzuki, R., Ohta, H., Yamori, T., Watanabe, M., Chun, J., and Arai, H. (2004). Lysophosphatidic acid and autotaxin stimulate cell motility of neoplastic and non-neoplastic cells through LPA1. J Biol Chem *279*, 17634-17639.

Hill, C.S., Wynne, J., and Treisman, R. (1995). The Rho family GTPases RhoA, Rac1, and CDC42Hs regulate transcriptional activation by SRF. Cell *81*, 1159-1170.

Horiuchi, A., Imai, T., Wang, C., Ohira, S., Feng, Y., Nikaido, T., and Konishi, I. (2003). Up-regulation of small GTPases, RhoA and RhoC, is associated with tumor progression in ovarian carcinoma. Lab Invest *83*, 861-870.

Igel, M., Sudhop, T., and von Bergmann, K. (2002). Pharmacology of 3-hydroxy-3-methylglutaryl-coenzyme A reductase inhibitors (statins), including rosuvastatin and pitavastatin. J Clin Pharmacol *42*, 835-845.

Ishii, I., Contos, J.J., Fukushima, N., and Chun, J. (2000). Functional comparisons of the lysophosphatidic acid receptors, LP(A1)/VZG-1/EDG-2, LP(A2)/EDG-4, and LP(A3)/EDG-7 in neuronal cell lines using a retrovirus expression system. Mol Pharmacol *58*, 895-902.

Jalink, K., Hengeveld, T., Mulder, S., Postma, F.R., Simon, M.F., Chap, H., van der Marel, G.A., van Boom, J.H., van Blitterswijk, W.J., and Moolenaar, W.H. (1995). Lysophosphatidic acid-induced Ca2+ mobilization in human A431 cells: structure-activity analysis. Biochem J *307 (Pt 2)*, 609-616.

Kaibuchi, K., Kuroda, S., and Amano, M. (1999). Regulation of the cytoskeleton and cell adhesion by the Rho family GTPases in mammalian cells. Annu Rev Biochem *68*, 459-486.

Karnoub, A.E., Symons, M., Campbell, S.L., and Der, C.J. (2004). Molecular basis for Rho GTPase signaling specificity. Breast Cancer Res Treat *84*, 61-71.

Kikuchi, T., Nagata, Y., and Abe, T. (1997). In vitro and in vivo antiproliferative effects of simvastatin, an HMG-CoA reductase inhibitor, on human glioma cells. J Neurooncol *34*, 233-239.

Kim, Y.M., and Benovic, J.L. (2002). Differential roles of arrestin-2 interaction with clathrin and adaptor protein 2 in G protein-coupled receptor trafficking. J Biol Chem *277*, 30760-30768.

Kue, P.F., Taub, J.S., Harrington, L.B., Polakiewicz, R.D., Ullrich, A., and Daaka, Y. (2002). Lysophosphatidic acid-regulated mitogenic ERK signaling in androgen-insensitive prostate cancer PC-3 cells. Int J Cancer *102*, 572-579.

Kusama, T., Mukai, M., Iwasaki, T., Tatsuta, M., Matsumoto, Y., Akedo, H., and Nakamura, H. (2001). Inhibition of epidermal growth factor-induced RhoA translocation and invasion of human pancreatic cancer cells by 3-hydroxy-3-methylglutaryl-coenzyme a reductase inhibitors. Cancer Res *61*, 4885-4891.

Lamaze, C., Chuang, T.H., Terlecky, L.J., Bokoch, G.M., and Schmid, S.L. (1996). Regulation of receptor-mediated endocytosis by Rho and Rac. Nature *382*, 177-179.

Lee, C.W., Rivera, R., Gardell, S., Dubin, A.E., and Chun, J. (2006). GPR92 as a new G12/13- and Gq-coupled lysophosphatidic acid receptor that increases cAMP, LPA5. J Biol Chem *281*, 23589-23597.

Lefkowitz, R.J. (2000). The superfamily of heptahelical receptors. Nat Cell Biol *2*, E133-136.

Lerner, E.C., Qian, Y., Blaskovich, M.A., Fossum, R.D., Vogt, A., Sun, J., Cox, A.D., Der, C.J., Hamilton, A.D., and Sebti, S.M. (1995). Ras CAAX peptidomimetic FTI-277 selectively blocks oncogenic Ras signaling by inducing cytoplasmic accumulation of inactive Ras-Raf complexes. J Biol Chem *270*, 26802-26806.

Leung, K.F., Baron, R., and Seabra, M.C. (2006). Thematic review series: lipid posttranslational modifications. geranylgeranylation of Rab GTPases. J Lipid Res *47*, 467-475.

Lin, S.X., Grant, B., Hirsh, D., and Maxfield, F.R. (2001). Rme-1 regulates the distribution and function of the endocytic recycling compartment in mammalian cells. Nat Cell Biol *3*, 567-572.

Linder, S., and Aepfelbacher, M. (2003). Podosomes: adhesion hot-spots of invasive cells. Trends Cell Biol *13*, 376-385.

Madaule, P., and Axel, R. (1985). A novel ras-related gene family. Cell *41*, 31-40.

Malecz, N., McCabe, P.C., Spaargaren, C., Qiu, R., Chuang, Y., and Symons, M. (2000). Synaptojanin 2, a novel Rac1 effector that regulates clathrin-mediated endocytosis. Curr Biol *10*, 1383-1386.

Mallard, F., Antony, C., Tenza, D., Salamero, J., Goud, B., and Johannes, L. (1998). Direct pathway from early/recycling endosomes to the Golgi apparatus revealed through the study of shiga toxin B-fragment transport. J Cell Biol *143*, 973-990.

Matar, P., Rozados, V.R., Binda, M.M., Roggero, E.A., Bonfil, R.D., and Scharovsky, O.G. (1999). Inhibitory effect of Lovastatin on spontaneous metastases derived from a rat lymphoma. Clin Exp Metastasis *17*, 19-25.

Maxfield, F.R., and McGraw, T.E. (2004). Endocytic recycling. Nat Rev Mol Cell Biol *5*, 121-132.

McGuire, T.F., Qian, Y., Vogt, A., Hamilton, A.D., and Sebti, S.M. (1996). Platelet-derived growth factor receptor tyrosine phosphorylation requires protein geranylgeranylation but not farnesylation. J Biol Chem *271*, 27402-27407.

Mellor, H., Flynn, P., Nobes, C.D., Hall, A., and Parker, P.J. (1998). PRK1 is targeted to endosomes by the small GTPase, RhoB. J Biol Chem *273*, 4811-4814.

Meyer zu Heringdorf, D., and Jakobs, K.H. (2007). Lysophospholipid receptors: signalling, pharmacology and regulation by lysophospholipid metabolism. Biochim Biophys Acta *1768*, 923-940.

Mills, G.B., and Moolenaar, W.H. (2003). The emerging role of lysophosphatidic acid in cancer. Nat Rev Cancer *3*, 582-591.

Miquel, K., Pradines, A., Sun, J., Qian, Y., Hamilton, A.D., Sebti, S.M., and Favre, G. (1997). GGTI-298 induces G0-G1 block and apoptosis whereas FTI-277 causes G2-M enrichment in A549 cells. Cancer Res *57*, 1846-1850.

Muck, A.O., Seeger, H., and Wallwiener, D. (2004). Inhibitory effect of statins on the proliferation of human breast cancer cells. Int J Clin Pharmacol Ther *42*, 695-700.

Mukai, M., Nakamura, H., Tatsuta, M., Iwasaki, T., Togawa, A., Imamura, F., and Akedo, H. (2000). Hepatoma cell migration through a mesothelial cell monolayer is inhibited by cyclic AMP-elevating agents via a Rho-dependent pathway. FEBS Lett *484*, 69-73.

Murph, M.M., Scaccia, L.A., Volpicelli, L.A., and Radhakrishna, H. (2003). Agonist-induced endocytosis of lysophosphatidic acid-coupled LPA_1/EDG-2 receptors via a Dynamin2- and Rab5-dependent pathway. J Cell Sci *116*, 1969-1980.

Murphy, C., Saffrich, R., Grummt, M., Gournier, H., Rybin, V., Rubino, M., Auvinen, P., Lutcke, A., Parton, R.G., and Zerial, M. (1996). Endosome dynamics regulated by a Rho protein. Nature *384*, 427-432.

Murphy, C., Saffrich, R., Olivo-Marin, J.C., Giner, A., Ansorge, W., Fotsis, T., and Zerial, M. (2001). Dual function of rhoD in vesicular movement and cell motility. Eur J Cell Biol *80*, 391-398.

Naslavsky, N., Boehm, M., Backlund, P.S., Jr., and Caplan, S. (2004a). Rabenosyn-5 and EHD1 interact and sequentially regulate protein recycling to the plasma membrane. Mol Biol Cell *15*, 2410-2422.

Naslavsky, N., Weigert, R., and Donaldson, J.G. (2004b). Characterization of a nonclathrin endocytic pathway: membrane cargo and lipid requirements. Mol Biol Cell *15*, 3542-3552.

Oakley, R.H., Laporte, S.A., Holt, J.A., Caron, M.G., and Barak, L.S. (2000). Differential affinities of visual arrestin, beta arrestin1, and beta arrestin2 for G protein-coupled receptors delineate two major classes of receptors. J Biol Chem *275*, 17201-17210.

Olofsson, B. (1999). Rho guanine dissociation inhibitors: pivotal molecules in cellular signalling. Cell Signal *11*, 545-554.

Paing, M.M., Stutts, A.B., Kohout, T.A., Lefkowitz, R.J., and Trejo, J. (2002). beta -Arrestins regulate protease-activated receptor-1 desensitization but not internalization or Down-regulation. J Biol Chem *277*, 1292-1300.

Paterson, H.F., Self, A.J., Garrett, M.D., Just, I., Aktories, K., and Hall, A. (1990). Microinjection of recombinant p21rho induces rapid changes in cell morphology. J Cell Biol *111*, 1001-1007.

Pereira-Leal, J.B., Hume, A.N., and Seabra, M.C. (2001). Prenylation of Rab GTPases: molecular mechanisms and involvement in genetic disease. FEBS Lett *498*, 197-200.

Pille, J.Y., Denoyelle, C., Varet, J., Bertrand, J.R., Soria, J., Opolon, P., Lu, H., Pritchard, L.L., Vannier, J.P., Malvy, C., Soria, C., and Li, H. (2005). Anti-RhoA and anti-RhoC siRNAs inhibit the proliferation and invasiveness of MDA-MB-231 breast cancer cells in vitro and in vivo. Mol Ther *11*, 267-274.

Pitcher, J.A., Freedman, N.J., and Lefkowitz, R.J. (1998). G protein-coupled receptor kinases. Annu Rev Biochem *67*, 653-692.

Presley, J.F., Mayor, S., Dunn, K.W., Johnson, L.S., McGraw, T.E., and Maxfield, F.R. (1993). The End2 mutation in CHO cells slows the exit of transferrin receptors from the recycling compartment but bulk membrane recycling is unaffected. J Cell Biol *122*, 1231-1241.

Qualmann, B., and Kessels, M.M. (2002). Endocytosis and the cytoskeleton. Int Rev Cytol *220*, 93-144.

Radeff-Huang, J., Seasholtz, T.M., Matteo, R.G., and Brown, J.H. (2004). G protein mediated signaling pathways in lysophospholipid induced cell proliferation and survival. J Cell Biochem *92*, 949-966.

Ridley, A. (2000). Rho GTPases. Integrating integrin signaling. J Cell Biol *150*, F107-109.

Ridley, A.J. (2001). Rho family proteins: coordinating cell responses. Trends Cell Biol *11*, 471-477.

Ridley, A.J. (2004). Rho proteins and cancer. Breast Cancer Res Treat *84*, 13-19.

Ridley, A.J., and Hall, A. (1992). The small GTP-binding protein rho regulates the assembly of focal adhesions and actin stress fibers in response to growth factors. Cell *70*, 389-399.

Ridley, A.J., Schwartz, M.A., Burridge, K., Firtel, R.A., Ginsberg, M.H., Borisy, G., Parsons, J.T., and Horwitz, A.R. (2003). Cell migration: integrating signals from front to back. Science *302*, 1704-1709.

Riento, K., and Ridley, A.J. (2003). Rocks: multifunctional kinases in cell behaviour. Nat Rev Mol Cell Biol *4*, 446-456.

Ruth, M.C., Xu, Y., Maxwell, I.H., Ahn, N.G., Norris, D.A., and Shellman, Y.G. (2006). RhoC promotes human melanoma invasion in a PI3K/Akt-dependent pathway. J Invest Dermatol *126*, 862-868.

Sahai, E., and Marshall, C.J. (2002). ROCK and Dia have opposing effects on adherens junctions downstream of Rho. Nat Cell Biol *4*, 408-415.

Schmid, S.L. (1997). Clathrin-coated vesicle formation and protein sorting: an integrated process. Annu Rev Biochem *66*, 511-548.

Schmidt, A., and Hall, A. (2002). Guanine nucleotide exchange factors for Rho GTPases: turning on the switch. Genes Dev *16*, 1587-1609.

Shao, F., and Dixon, J.E. (2003). YopT is a cysteine protease cleaving Rho family GTPases. Adv Exp Med Biol *529*, 79-84.

Sheff, D.R., Daro, E.A., Hull, M., and Mellman, I. (1999). The receptor recycling pathway contains two distinct populations of early endosomes with different sorting functions. J Cell Biol *145*, 123-139.

Shenoy, S.K., and Lefkowitz, R.J. (2003). Multifaceted roles of beta-arrestins in the regulation of seven-membrane-spanning receptor trafficking and signalling. Biochem J *375*, 503-515.

Shenoy, S.K., McDonald, P.H., Kohout, T.A., and Lefkowitz, R.J. (2001). Regulation of receptor fate by ubiquitination of activated beta 2-adrenergic receptor and beta-arrestin. Science *294*, 1307-1313.

Song, J., Khachikian, Z., Radhakrishna, H., and Donaldson, J.G. (1998). Localization of endogenous ARF6 to sites of cortical actin rearrangement and involvement of ARF6 in cell spreading. J Cell Sci *111 (Pt 15)*, 2257-2267.

Stam, J.C., Michiels, F., van der Kammen, R.A., Moolenaar, W.H., and Collard, J.G. (1998). Invasion of T-lymphoma cells: cooperation between Rho family GTPases and lysophospholipid receptor signaling. Embo J *17*, 4066-4074.

Stark, W.W., Jr., Blaskovich, M.A., Johnson, B.A., Qian, Y., Vasudevan, A., Pitt, B., Hamilton, A.D., Sebti, S.M., and Davies, P. (1998). Inhibiting geranylgeranylation blocks growth and promotes apoptosis in pulmonary vascular smooth muscle cells. Am J Physiol *275*, L55-63.

Su, Y., Raghuwanshi, S.K., Yu, Y., Nanney, L.B., Richardson, R.M., and Richmond, A. (2005). Altered CXCR2 signaling in beta-arrestin-2-deficient mouse models. J Immunol *175*, 5396-5402.

Sun, J., Qian, Y., Hamilton, A.D., and Sebti, S.M. (1998). Both farnesyltransferase and geranylgeranyltransferase I inhibitors are required for inhibition of oncogenic K-Ras prenylation but each alone is sufficient to suppress human tumor growth in nude mouse xenografts. Oncogene *16*, 1467-1473.

Suwa, H., Ohshio, G., Imamura, T., Watanabe, G., Arii, S., Imamura, M., Narumiya, S., Hiai, H., and Fukumoto, M. (1998). Overexpression of the rhoC gene correlates with progression of ductal adenocarcinoma of the pancreas. Br J Cancer *77*, 147-152.

Symons, M., and Rusk, N. (2003). Control of vesicular trafficking by Rho GTPases. Curr Biol *13*, R409-418.

Teo, M., Tan, L., Lim, L., and Manser, E. (2001). The tyrosine kinase ACK1 associates with clathrin-coated vesicles through a binding motif shared by arrestin and other adaptors. J Biol Chem *276*, 18392-18398.

Toews, M.L., Ustinova, E.E., and Schultz, H.D. (1997). Lysophosphatidic acid enhances contractility of isolated airway smooth muscle. J Appl Physiol *83*, 1216-1222.

Ullrich, O., Reinsch, S., Urbe, S., Zerial, M., and Parton, R.G. (1996). Rab11 regulates recycling through the pericentriolar recycling endosome. J Cell Biol *135*, 913-924.

Urs, N.M., Jones, K.T., Salo, P.D., Severin, J.E., Trejo, J., and Radhakrishna, H. (2005). A requirement for membrane cholesterol in the beta-arrestin- and clathrin-

dependent endocytosis of LPA1 lysophosphatidic acid receptors. J Cell Sci *118*, 5291-5304.

van Corven, E.J., van Rijswijk, A., Jalink, K., van der Bend, R.L., van Blitterswijk, W.J., and Moolenaar, W.H. (1992). Mitogenic action of lysophosphatidic acid and phosphatidic acid on fibroblasts. Dependence on acyl-chain length and inhibition by suramin. Biochem J *281 (Pt 1)*, 163-169.

van der Sluijs, P., Hull, M., Webster, P., Male, P., Goud, B., and Mellman, I. (1992). The small GTP-binding protein rab4 controls an early sorting event on the endocytic pathway. Cell *70*, 729-740.

van Leeuwen, F.N., Giepmans, B.N., van Meeteren, L.A., and Moolenaar, W.H. (2003). Lysophosphatidic acid: mitogen and motility factor. Biochem Soc Trans *31*, 1209-1212.

Veillard, N.R., and Mach, F. (2002). Statins: the new aspirin? Cell Mol Life Sci *59*, 1771-1786.

Vogt, A., Qian, Y., McGuire, T.F., Hamilton, A.D., and Sebti, S.M. (1996). Protein geranylgeranylation, not farnesylation, is required for the G1 to S phase transition in mouse fibroblasts. Oncogene *13*, 1991-1999.

Vogt, A., Sun, J., Qian, Y., Hamilton, A.D., and Sebti, S.M. (1997). The geranylgeranyltransferase-I inhibitor GGTI-298 arrests human tumor cells in G0/G1 and induces p21(WAF1/CIP1/SDI1) in a p53-independent manner. J Biol Chem *272*, 27224-27229.

Wallar, B.J., and Alberts, A.S. (2003). The formins: active scaffolds that remodel the cytoskeleton. Trends Cell Biol *13*, 435-446.

Wang, D.A., Lorincz, Z., Bautista, D.L., Liliom, K., Tigyi, G., and Parrill, A.L. (2001). A single amino acid determines lysophospholipid specificity of the S1P1 (EDG1) and LPA1 (EDG2) phospholipid growth factor receptors. J Biol Chem *276*, 49213-49220.

Wolfe, B.L., and Trejo, J. (2007). Clathrin-dependent mechanisms of G protein-coupled receptor endocytosis. Traffic *8*, 462-470.

Wu, M., Wu, Z.F., Kumar-Sinha, C., Chinnaiyan, A., and Merajver, S.D. (2004). RhoC induces differential expression of genes involved in invasion and metastasis in MCF10A breast cells. Breast Cancer Res Treat *84*, 3-12.

Xiao, K., Garner, J., Buckley, K.M., Vincent, P.A., Chiasson, C.M., Dejana, E., Faundez, V., and Kowalczyk, A.P. (2005). p120-Catenin regulates clathrin-dependent endocytosis of VE-cadherin. Mol Biol Cell *16*, 5141-5151.

Xu, Y., Fang, X.J., Casey, G., and Mills, G.B. (1995). Lysophospholipids activate ovarian and breast cancer cells. Biochem J *309 (Pt 3)*, 933-940.

Zalcman, G., Closson, V., Linares-Cruz, G., Lerebours, F., Honore, N., Tavitian, A., and Olofsson, B. (1995). Regulation of Ras-related RhoB protein expression during the cell cycle. Oncogene *10*, 1935-1945.

Zhang, J., Barak, L.S., Anborgh, P.H., Laporte, S.A., Caron, M.G., and Ferguson, S.S. (1999). Cellular trafficking of G protein-coupled receptor/beta-arrestin endocytic complexes. J Biol Chem *274*, 10999-11006.

Zhang, J., Ferguson, S.S., Barak, L.S., Aber, M.J., Giros, B., Lefkowitz, R.J., and Caron, M.G. (1997). Molecular mechanisms of G protein-coupled receptor signaling: role of G protein-coupled receptor kinases and arrestins in receptor desensitization and resensitization. Receptors Channels *5*, 193-199.

Zong, H., Raman, N., Mickelson-Young, L.A., Atkinson, S.J., and Quilliam, L.A. (1999). Loop 6 of RhoA confers specificity for effector binding, stress fiber formation, and cellular transformation. J Biol Chem *274*, 4551-4560.